

THESIS FOR THE DEGREE OF DOCTOR OF PHILOSOPHY
IN
THERMO AND FLUID DYNAMICS

**Multi-objective CFD-based
design method for axial
compressors**

LARS ELLBRANT

Division of Fluid Dynamics

Department of Applied Mechanics

CHALMERS UNIVERSITY OF TECHNOLOGY

Göteborg, Sweden, 2014

**Multi-objective CFD-based design method for axial com-
pressors**

LARS ELLBRANT

ISBN 978-91-7597-069-1

© LARS ELLBRANT, 2014

Doktorsavhandling vid Chalmers tekniska högskola

Ny serie nr 3750

ISSN 0346-718X

Division of Fluid Dynamics

Department of Applied Mechanics

Chalmers University of Technology

SE-412 96 Göteborg, Sweden

Phone: +46-(0)31-7721000

Fax: +46-(0)31-7723872

Printed at Chalmers Reproservice
Göteborg, Sweden, 2014

Multi-objective CFD-based design method for axial compressors

LARS ELLBRANT

Division of Fluid Dynamics
Department of Applied Mechanics
Chalmers University of Technology

Abstract

Economic aspects such as reducing specific fuel consumption and ever growing environmental requirements on emissions and perceived noise levels are the major incentives in the pursuit to improve aircraft engines. The overall efficiency of the engine is a combination of propulsive efficiency and thermal efficiency. A new, promising engine concept with very high propulsive efficiency is the so-called Open Rotor. In order to facilitate high thermal efficiency, the core of the engine must be designed with a high turbine inlet temperature as well as a high overall pressure ratio in combination with being light and compact. For the low-pressure compression system, the desire to reduce weight leads to a reduction of the number of stages. This must be realized by a combination of high transonic rotor speeds and high stage loadings in order to maintain the required pressure ratio. However, this becomes a tough design challenge aerodynamically as it will be more difficult to design the compressor with respect to high efficiency and sufficient stability along the entire operating line. This thesis presents a new design methodology, accounting for both efficiency and stability. The optimal set of solutions in the multi-objective space is explored with help of CFD computations integrated with an optimization framework that consists of a meta-model assisted genetic algorithm. In order to utilize the design process for industrial applications, the reductions in total design time and computational resources are also addressed. The validity of the analysis method developed is assessed by means of experimental data obtained from three transonic, highly loaded compressor cases including a rotor in isolation, a rotor-stator configuration and a three stage compressor.

Keywords: Turbomachinery, Compressor, Transonic, Design, Validation, CFD, Q3D, Optimization, Meta-modeling

List of Publications

This thesis is based on the work contained in the following papers:

- I L. Ellbrant, L-E. Eriksson and H. Mårtensson, 2011, CFD Validation of a High Speed Transonic 3.5 Stage Axial Compressor, *20th ISABE Conference, ISABE-2011-1226*, September 12-16, Gothenburg, Sweden
- II L. Ellbrant, L-E. Eriksson and H. Mårtensson, 2012, Design of Compressor Blades Considering Efficiency and Stability Using CFD Based Optimization, *Proceedings of ASME Turbo Expo, GT2012-69272*, June 11-15, Copenhagen, Denmark
- III L. Ellbrant, L-E. Eriksson and H. Mårtensson, 2012, CFD Optimization of a Transonic Compressor Using Multiobjective GA and Metamodels, *28th ICAS Conference*, September 23-28, Brisbane, Australia
- IV L. Ellbrant, L-E. Eriksson and H. Mårtensson, 2013, Balancing Efficiency and Stability In the Design of Transonic Compressor Stages, *Proceedings of ASME Turbo Expo, GT2013-94838*, June 3-7, San Antonio, Texas, USA
- V L. Ellbrant, L-E. Eriksson and H. Mårtensson, 2013, Aerodynamic Properties of Novel Compressor Blade Shapes, *21st ISABE Conference, ISABE-2013-1103*, September 9-13, Busan, Korea
- VI L. Ellbrant, L-E. Eriksson and H. Mårtensson, 2014, Predictive Capability of CFD Models for Transonic Compressor Design, *Proceedings of ASME Turbo Expo, GT2014-27019*, June 16-20, Düsseldorf, Germany
- VII L. Ellbrant, L-E. Eriksson, 2014, General 3D Streamtube Solver, *Internal report*, Dept. of Applied Mechanics, Chalmers University of Technology, Gothenburg, Sweden, to be published.

Acknowledgments

This work was funded by the Swedish National Aviation Engineering Research Programme, NFFP. The author would like to acknowledge the financial support of VINNOVA, the Swedish Defense Material Administration (FMV) and GKN Aerospace Engine Systems. Furthermore, the National Supercomputer Center, Linköping, Sweden and Chalmers Center for Computational Science and Engineering, Gothenburg, Sweden are acknowledged for providing the computational resources required for this work.

I would first like to thank my supervisor Lars-Erik Eriksson for sharing his knowledge and ideas with me. His support and guidance over the past five years have been extremely helpful. I would also like to thank Hans Mårtensson at GKN Aerospace for his technical support and for our many interesting discussions in the field of compressor aerodynamics. With the combined knowledge from Lars-Erik and Hans, I have rarely stumbled upon a question that has been left unanswered. Furthermore I would like to direct a special thanks to the compressor design-team at GKN Aerospace. The feedback I have received has been very valuable and our discussions are greatly appreciated. Many thanks to all my friends and colleagues at the division of Fluid Dynamics at Chalmers. The time at the division has been really nice and memorable, everything from the “deep” discussions at the lunch breaks (which for some reason tend to lead to the concept of “bicycle-tunnels”) to the annual Christmas party. I would also like to thank Niklas Andersson for his assistance and feedback on this thesis. I am also thankful to Monica Vargman and Ulla Lindberg-Thieme for the administrative help I have received. Finally, I would like to thank Sofia for her support and I am very impressed by her patience when my work hours rapidly increased, almost discontinuously, followed by high losses in availability.

*If everything seems to be going well,
you have obviously overlooked something.
- Murphy's Law*

Nomenclature

Roman

C	velocity in the absolute frame
C_p	specific heat capacity at constant pressure
C_v	specific heat capacity at constant volume
e	internal energy
h	enthalpy
k	turbulence kinetic energy
P, p	pressure
Pr	laminar Prandtl number
Pr_t	turbulent Prandtl number
R	gas constant, degree of reaction
r	radial coordinate
T	temperature
t	thickness, time
U	blade wheelspeed
u_i	velocity vector in Cartesian coordinates
V	velocity in the relative frame
v	camber

Greek Symbols

α	absolute flow angle, metal angle
β	relative flow angle
γ	specific heat ratio, stagger angle
δ_{ij}	Kronecker delta
ε	turbulence dissipation
η	polytropic efficiency
θ	tangential coordinate
μ	laminar dynamic viscosity, wedge angle

μ_t	turbulent eddy viscosity
ρ	density
τ_{ij}	viscous stress tensor
ϕ	flow coefficient
ψ	work coefficient

Subscripts

0	total condition
le	leading edge
m	meridional coordinate
te	trailing edge

Miscellaneous Symbols

$\bar{}$	ensemble average
$\tilde{}$	Favre averaged (density weighed averages)

Abbreviations

CFD	Computational Fluid Dynamics
DOE	Design Of Experiment
GA	Genetic Algorithm
RANS	Reynolds Averaged Navier-Stokes
RBF	Radial Basis Function
RSM	Response Surface Model
Q3D	Quasi-3D

Contents

Abstract	iii
List of Publications	v
Acknowledgments	vii
Nomenclature	xi
1 Introduction	1
1.1 Motivation	1
1.2 Scope of work	4
2 Design procedure	5
2.1 Overall requirements	5
2.2 Levels of design	6
2.2.1 Thermodynamic design	7
2.2.2 Throughflow design	9
2.2.3 CFD design	10
2.3 Blade parameterization	13
3 CFD modeling	19
3.1 Governing equations	19
3.1.1 Discretization	21
3.2 Geometry representation	22
3.2.1 Tip clearance	22
3.3 Computational domain	23
3.4 Boundary conditions	23
3.4.1 Mixing planes	25
3.5 Mesh sensitivity study	25
3.6 Turbulence modeling	26
4 Optimization	29
4.1 Deterministic methods	29

4.2	Non-deterministic methods	31
4.3	Selection of optimization algorithm	32
4.4	Meta-models	32
4.4.1	Radial Basis Functions	33
4.5	On the selection of meta-model	34
4.6	Developed optimization framework	35
5	Summary of Papers	37
5.1	Paper I	37
5.1.1	Division of Work	37
5.1.2	Results and Discussion	37
5.2	Paper II	38
5.2.1	Division of Work	38
5.2.2	Results and Discussion	38
5.3	Paper III	39
5.3.1	Division of Work	39
5.3.2	Results and Discussion	39
5.4	Paper IV	40
5.4.1	Division of Work	40
5.4.2	Results and Discussion	40
5.5	Paper V	41
5.5.1	Division of Work	41
5.5.2	Results and Discussion	41
5.6	Paper VI	42
5.6.1	Division of Work	42
5.6.2	Results and Discussion	42
5.7	Paper VII	43
5.7.1	Division of Work	43
5.7.2	Results and Discussion	43
6	Concluding Remarks	45
6.1	Validation	45
6.2	Design procedure	46
6.3	Optimization	46
6.4	Future work	47
	Bibliography	48

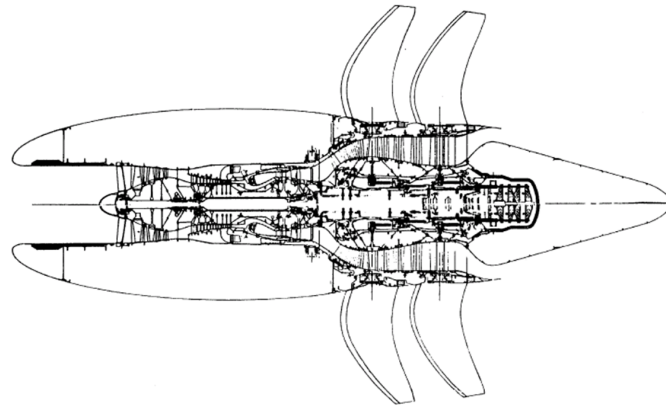
Chapter 1

Introduction

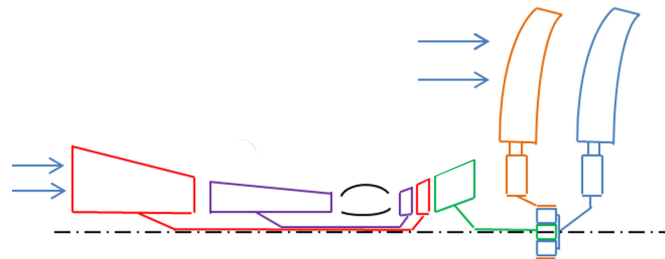
1.1 Motivation

Economic aspects, such as reductions in specific fuel consumption and ever growing environmental requirements on emissions and perceived noise levels, are the major drivers in improving aircraft engines. The most common type of engine used for commercial flight is the turbofan engine. The overall efficiency of the engine is a combination of propulsive efficiency and thermal efficiency. The thermal efficiency describes the efficiency of the process in which the energy contained in the fuel is converted into kinetic energy while the propulsive efficiency is a measure of the proportion of the available kinetic energy that is used to produce useful thrust. As described in Saravanamutto *et al.* (2009), the propulsive efficiency may be improved by increasing the mass flow through the engine while decreasing the difference between the flight speed and the engine jet speed. A new, promising engine concept with very high propulsive efficiency is the so-called Open Rotor. In short, the high mass flow and low velocity difference is facilitated by the use of un-ducted fans with a large diameter and low fan pressure ratio. Some attempts to realize this concept were made as early as in the 1980s. GE Aircraft Engines (1987) describes the design and test done at General Electric. The concept was abandoned, however, most likely due to unresolved technical issues such as noise and reduced fuel prices leading to a reduction of its commercial advantage. Nevertheless, because of today's great environmental concerns and the steady increase in oil prices, the Open Rotor has become one of the most promising solutions. The cross-sectional view of the engine architecture used in GE Aircraft Engines (1987) is shown in Fig. 1.1(a) where the gas generator

is a slightly modified F404 connected to a power turbine propelling the un-ducted fans. Alternative architectures are currently being investigated. One of the most promising concepts, studied in Larsson (2014), is shown in Fig. 1.1(b). The main difference between the two engines



(a) Constructed by GE in GE Aircraft Engines (1987)



(b) Studied at Chalmers in Larsson (2014)

Figure 1.1: Alternatives of Open Rotor configurations

presented above is the way in which the power turbine is connected to the fans. The gearbox seen in Fig. 1.1(b) adds additional weight and, due to its complexity, is likely to require more maintenance. However, the turbine design for this concept can be designed to operate more optimal as it is not limited to the low rotational speed imposed by the fans. This leads to fewer stages and thus a lighter turbine. What is common for both approaches is that the core consists of a two-shaft gas generator. In order to successfully meet the stringent environmental requirements, the core is required to have high thermal efficiency as well as being light and compact. The high thermal efficiency is accomplished by having a high combustor outlet temperature and high overall pressure ratio. Concerning the low pressure compression system, the desire to reduce the weight leads to a reduction in the number of stages. In order to maintain the required pressure ratio, this must be realized by a combination of high transonic rotor speeds and high

stage loadings. This unfortunately leads to a challenging design task aerodynamically as it will be more difficult to design the compressor with respect to high efficiency as well as high stability along the entire operating line. Moreover a concern, specifically for the architecture shown in Fig. 1.1(a), has been the change in the operating line of the low-pressure compressor caused by the compatibility requirement of the additional power turbine, presented in Fig. 1.2. The operating line

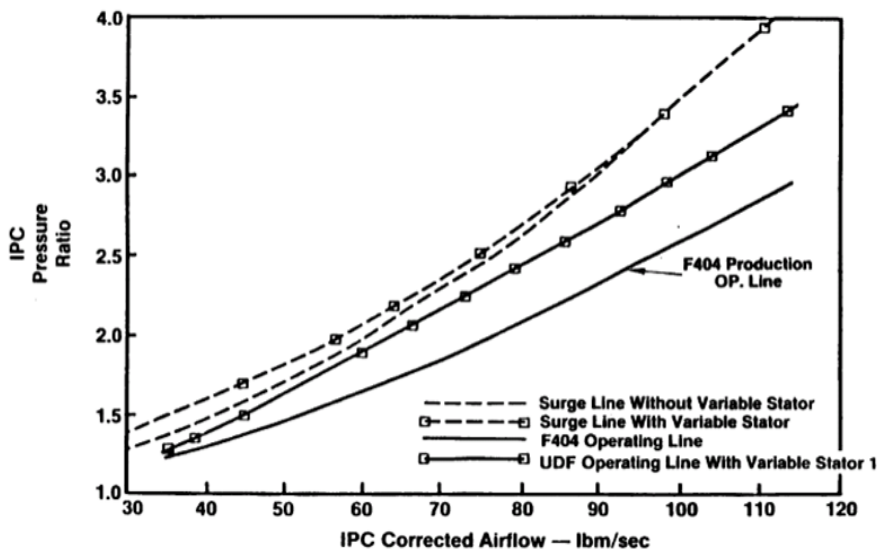


Figure 1.2: Low pressure compressor map characteristic including the operating lines represented by the nominal and the Open Rotor engines, GE Aircraft Engines (1987)

of the Open Rotor, also known as the UDF, is much steeper compared to the original operating line of the F404, which results in a relatively low stall margin at part speed. Whether or not this effect is present in the current studied configurations is not known, but the results shown in Fig. 1.2 indicate that stability in particular at part speed may become even more critical for engines of this type. Traditional aerodynamic design methods for low-pressure compressors have been focused on improving the design point efficiency. However, due to the part speed stability issues seen in Fig. 1.2 in combination with the general trend of increasing pressure ratio and reduced weight of the compressor module, a new design method is required where stability can be considered early in the design process.

1.2 Scope of work

This thesis centers around a new aerodynamic design methodology for axial compressors. The primary objective has been to construct an efficient CFD-based compressor design procedure that has the ability to balance high efficiency with high stability. To reach this objective the following subtasks were carried out:

Validation of the CFD model in order to assess the capability to predict the overall compressor performance. The main focus of this sub task was to build a sufficiently accurate CFD model that is still fast enough to be suitable for optimization purposes.

Build an efficient optimization framework that is able to handle multi-objective constraint problems. This work included selecting a suitable meta-model that effectively reduces the number of CFD computations required.

Verify the design procedure by re-designing a highly loaded transonic compressor stage which should be compatible with a multi-stage environment.

Chapter 2

Design procedure

2.1 Overall requirements

The overall requirements for a compressor are set by the engine cycle, which in turn has been optimized to match a specific aircraft and mission. From an aerodynamic perspective, the major requirements include the compressor pressure ratio, flow capacity, desired efficiency and operability but also indirectly the desired weight, which influences the selection of the number of stages. The overall compressor design characteristics are commonly presented in the form of a compressor map as illustrated in Fig. 2.1. This map may be obtained from CFD predictions during the design phase, but the final map is likely to be verified by rig testing. The performance is measured in terms of the variation of total pressure ratio and efficiency at different mass flow rates. The speedlines marked in the map represent the compressor performance at constant rotational speeds. In the region where the speedlines are vertical, the compressor is choked. As the throttle valve of the rig is closed, the exit pressure increases forcing the compressor to operate at a higher pressure ratio. Once the compressor becomes un-choked, the pressure ratio increase is also associated with a reduction in mass flow. At some point during this operation, the compressor becomes unstable, and closing the throttle further will result in stall or surge. The working line shown in Fig. 2.1 represents the steady state operation of the compressor in the engine environment at different rotational speeds. The crossing between the working line and the design rotational speed defines the compressor design point where the required overall pressure ratio, mass flow and efficiency should be fulfilled. The required operability is commonly referred to as the stall

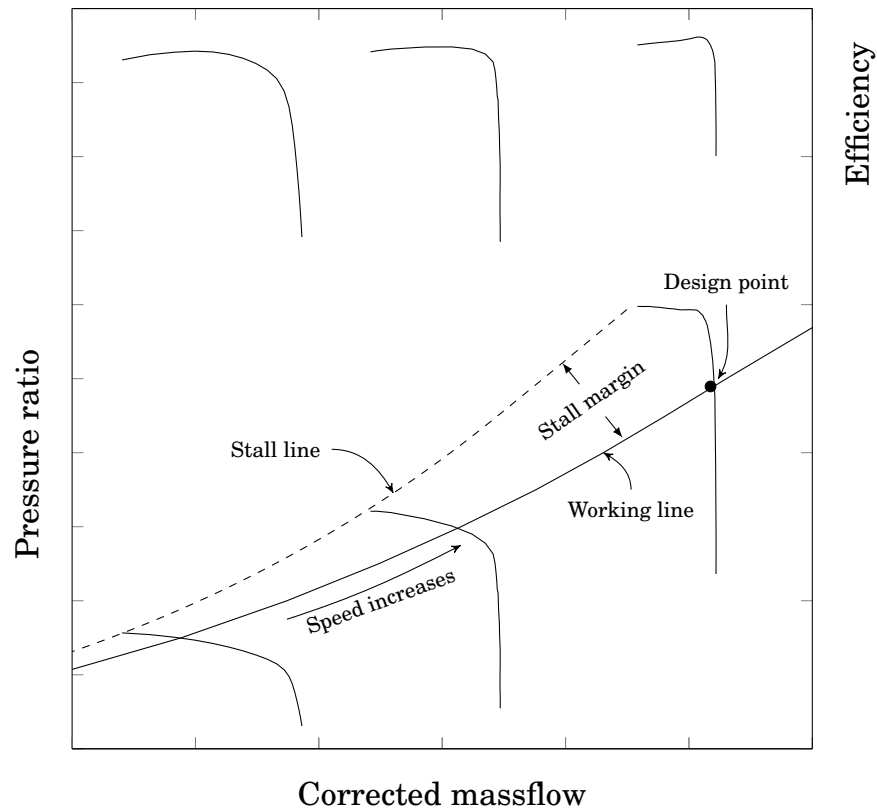


Figure 2.1: Typical compressor map

margin and is related to the distance between the working line and the stall limit. The stall margin must be sufficiently large to cover transient operations that force the compressor to deviate from the working line as well as other effects such as inlet distortion, real geometry effects and a deterioration of performance over time.

2.2 Levels of design

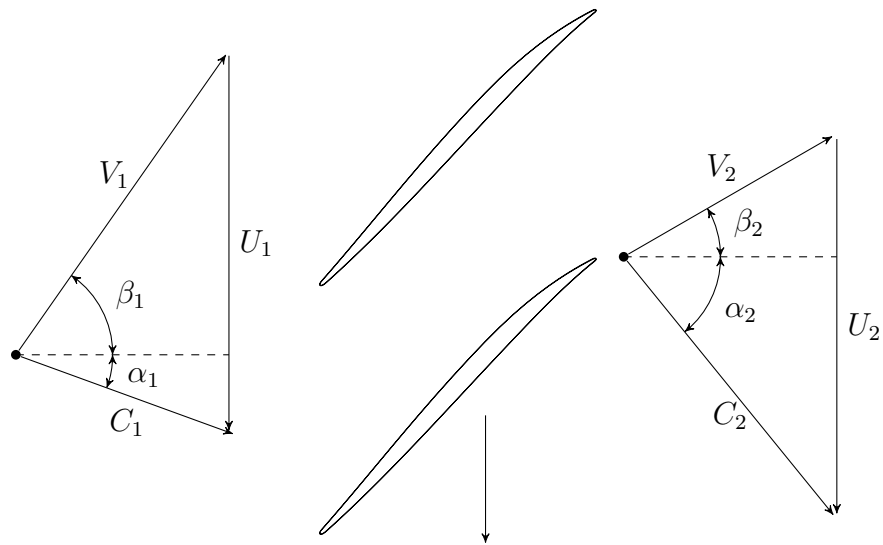
The design procedure for a compressor from cycle performance to the three-dimensional design of blade shapes is very complex and involves many disciplines. Since the compressor is one of the main components in an aircraft engine defining its overall performance characteristics, the design philosophy and information on the design work flow is to a large extent proprietary but general guidelines may be found in many textbooks and reports such as Johnsen & Bullock (1965), Cumpsty (1989) and McKenzie (1997). The purpose of the following is to give the reader an overview of the procedure and to put the present work

into the context of the whole design chain related to the aerodynamic discipline. The complete description of the flow in a compressor is very complex. In essence, the flow is unsteady and three-dimensional where turbulence, viscous and compressible effects play a major role. Up to the present there has been no CFD method that has the ability to fully capture this flow while being computationally cheap enough to be feasible for design purposes. Instead, simplified forms of the governing equations have been considered. With regard to design methods, the degree of complexity of the analysis model may be divided into three main stages in which different aspects of the design space can be considered.

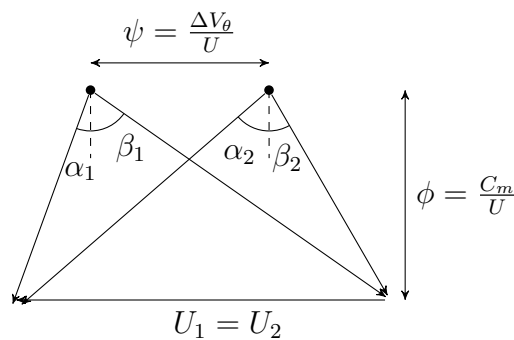
2.2.1 Thermodynamic design

The first stage consists of determining the overall layout of the compressor. Regarding the rotational speed, the upper limit is typically set by the relative tip Mach number in order to avoid high shock losses and reduced operability. However, this speed may lead to too high stress on the turbine disk, so the decision needs to be balanced with requirements set on the turbine. The overall dimensions such as length, inner and outer radii are based on the weight requirements and the available space within the engine. These parameters also have a significant impact on the aerodynamic performance as they affect the selection of the number of stages in the compressor as well as the hub-to-tip ratio and aspect ratio of the blade rows. Furthermore, mechanical constraints limit the axial gaps between blade rows and must be considered as well. The aerodynamic design is typically performed along the meridional streamline positioned at the mean radius. The most fundamental design choice is the velocity triangles in and out from each stage as depicted in Fig. 2.2(a). To illustrate the most important parameters, a simplified example is shown in Fig. 2.2(b) in which a constant axial velocity as well as a constant radius through the blade row are assumed. The velocity triangles are normalized with the blade speed (U) and are described in terms of the flow coefficient (ϕ), the work coefficient (ψ) and the degree of reaction (R), defined in Eqn. 2.1.

$$\begin{aligned}
 \phi &= \frac{C_m}{U} \\
 \psi &= \frac{\Delta h_0}{U^2} \\
 R &= \frac{\Delta h_{rotor}}{\Delta h_{stage}}
 \end{aligned}
 \tag{2.1}$$



(a) Velocity triangles in and out from a rotor along a streamline



(b) Velocity triangles normalized with U

Figure 2.2: Preliminary design

The degree of reaction is a measure of how much of the diffusion that occurs in the rotor relative to the whole stage. Traditionally the diffusion has been equally divided between the rotor and stator, Cumpsty (1989), but the more recent study of Dickens & Day (2009) found that increasing the diffusion in the rotor for highly loaded compressors increased the efficiency. The inlet flow coefficient must be selected to be consistent with the required flow capacity. The work coefficient is related to the Euler equation for turbomachinery as shown in Eqn. 2.2 for the special case of constant radius, that is illustrated in Fig.

2.2(b).

$$\begin{aligned}
 \Delta h_0 &= U_2 V_{\theta 2} - U_1 V_{\theta 1} \\
 \Rightarrow \Delta h_0 &= U \Delta V_{\theta} \\
 \Rightarrow \frac{\Delta h_0}{U^2} &= \frac{\Delta V_{\theta}}{U} \\
 \Rightarrow \frac{\Delta h_0}{U^2} &= \psi
 \end{aligned} \tag{2.2}$$

It can be used to determine the number of blade rows needed to obtain the required total pressure ratio provided that an assumption is made on the efficiency. Increasing the work coefficient leads to fewer blade rows and thus may reduce weight and length of the compressor, but it is also directly related to an increased aerodynamic design challenge as it will be more difficult to obtain the required efficiency and operability. Although the work coefficient gives an indication of the pressure ratio, it is not directly linked to the aerodynamic difficulties involved. To this end, the well known Diffusion factor developed in Lieblein (1959) can be used to set an appropriate blade solidity given that the velocity triangles have been determined, shown in Eqn. 2.3

$$DF = 1 - \frac{V_2}{V_1} + \frac{\Delta V_{\theta}}{2\sigma V_1} \tag{2.3}$$

where the blade solidity (σ) is equal to the ratio between blade chord and blade pitch. Common practice is to use a Diffusion factor of 0.45 at the design point, Cumpsty (1989). The efficiency of the blade row at this stage is calculated with correlations of profile losses and deviation.

2.2.2 Throughflow design

In the next design stage a throughflow method is commonly used to determine the radial matching of each blade row as well as the stage matching of the compressor. An important aspect to consider is that the flow velocities at different radial positions are interconnected by the radial equilibrium of the flow, Cumpsty (1989). The most popular approach is to consider a streamline curvature method based on the general S1/S2 theory outlined by C. H. Wu (1952). The basis of the procedure is to consider the full radial equilibrium equation using the assumption that the flow may be treated as inviscid and axisymmetrical. The flowfield in the meridional plane (S2) is then obtained along streamlines, visualized in Fig. 2.3, where the influence

of the blades is accounted for by introducing blade models. The presence of the blades may be described by empirical models that have been summarized in Aungier (2003) among others. Alternative techniques account for the blade mean geometry in the meridional flow solver, as described in Baralon *et al.* (1998) or Casey & Robinson (2010). The work in Spurr (1980) successfully coupled the meridional solver to a Q3D solver that obtains the flow solution in the blade-to-blade plane (S1) and, by iterating between the two solvers, managed to improve the accuracy of the performance predictions. As described in Aungier (2003), correlations are frequently used for profile losses, shock losses and tip clearance losses, and blockage factors are employed at endwalls and blades to account for the effect of boundary layers.

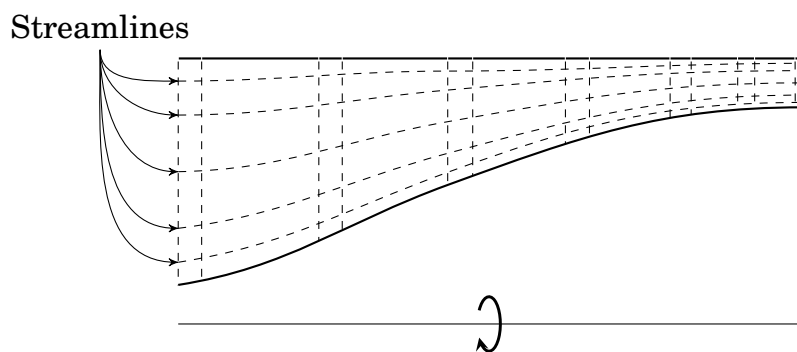


Figure 2.3: 2D design space

2.2.3 CFD design

Once the compressor layout from the throughflow method agrees with the desired performance, a considerable effort remains to define corresponding blade geometries. In contrast to the previous design stages, the CFD-based method requires much more computational resources; thus an efficient design rationale needs to be considered. A common approach is to first optimize each multistage compressor component in isolation using boundary conditions originating from the streamline curvature analysis. This is typically done by first optimizing the 2D profiles along the blade span using a blade-to-blade solver. The selected profiles are then stacked together to form an initial 3D blade, which can then be optimized further in 3D. Several approaches to single blade row optimizations have been published, for instance in the work of Oyama *et al.* (2004), Swoboda *et al.* (2008) and Luo *et al.* (2009).

However, these methods may be of limited use when designing multi-stage compressors. The main reason is the difficulty of specifying a well-posed boundary condition at the outlet that is representative of the multi-stage environment. Furthermore, an optimization of a single rotor could lead to difficulties in the stator design, unless properly constrained. For instance, if the optimal rotor blade outlet Mach number levels are high, the stator losses could be excessive; this would lead to a non-optimal stage performance, as discussed in the work of Okui *et al.* (2013). Optimizations of single or multiple stages eliminate some of these problems and have been shown to be successful. The work described in Aulich & Siller (2011) presented a 3D optimization procedure for a fan stage starting from a baseline 3D geometry. Similarly, the work of Bonaiuti & Zangeneh (2009) describes an efficient method to improve a compressor stage by the use of 3D optimization. Because of the high dimensional design space involved in 3D design it is however important to start these types of optimizations from a baseline geometry in order to keep the computational resources to a manageable size. In the present work, the overall requirements set on the whole compressor are distributed into requirements for the individual stages rather than for each component separately. This is done by extracting the flow properties of each stage from the throughflow solution or, if available, from a baseline 3D CFD analysis. The basis of the methodology then consists of optimizing the stages separately. The design strategy for each stage, shown in Fig 2.4, is divided into two steps. To limit the 3D design space describing the rotor and stator geometry, the optimization is first done along three streamtubes using a Q3D solver in which the rotor and stator profiles are determined. The Q3D solver has traditionally been based on the assumption of inviscid flow, such as outlined in McFarland (1984) and Bölcs & Tsamourtzis (1991). The viscous effect has also been incorporated by the introduction of the displacement thickness concept, and this type of solver has found wide usage for designing blade profiles. In Köller *et al.* (2000) the Q3D inviscid/viscous solver MISES developed by Youngreen & Drela (1991) was used to optimize compressor profiles with the purpose of creating a new profile family. In the work of Schmitz *et al.* (2011) the Q3D solver was used to predict total pressure loss and flow-turning for a wide range of different compressor profile shapes. This large database was then used to obtain improved correlations of the blade performance model in their streamline curvature solver. In the present work, however, a new Q3D solver is suggested. The main idea is to use the 3D CFD solver on “thin layer” computational grids resolving the 3D streamtube blade-to-blade domain. The same type of CFD settings may then be

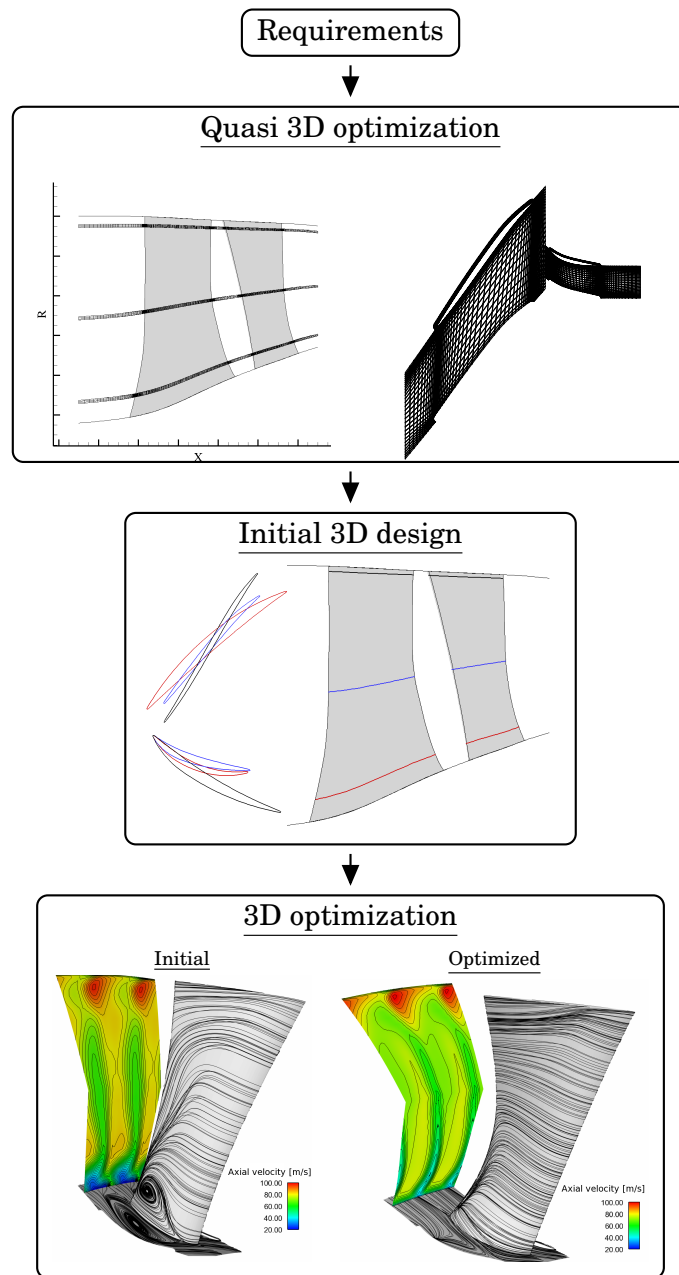


Figure 2.4: Design strategy

used, e.g. boundary conditions, turbulence model and interfaces, such as the mixing plane implementation allowing the Q3D method to solve for rotor-stator configurations. Furthermore, by considering the full 3D streamtube, the radius, area and flow angle variations are all preserved along the blade passage. The main issue with this approach is a slightly higher computational cost relative to the simplified 2D

blade-to-blade methods. However, by introducing a source term that reproduces the pressure gradient normal to the streamtube, it is possible to use single-layer grids; thus the computational cost can be kept low. The advantage of the new approach is that the method is less dependent on correlations and more closely related to a 3D CFD model in terms of physical modeling. Provided that the streamtubes are a fair approximation to the 3D flow, the initial stage will be an appropriate base geometry and, as such, the 3D stage optimization becomes less time consuming. In the final step, the 3D optimization is used to pursue additional improvements in performance by utilizing not only design parameters describing the profile shape but also by modifying the stacking line to allow for lean and sweep.

2.3 Blade parameterization

Before CFD methods were utilized as design tools, blade profiles were selected from various families of airfoils such as the NACA 65 series, the British C series and the double circular arc (DCA), see Cumpsty (1989). Correlations for the performance characteristics of these blade families, obtained by extensive experimental cascade testing, were used to select an appropriate profile. However, with the advent of improved computing capability, it is now possible to investigate free-form blade profiles rather than being restricted to certain families of blades. Free-form profiles, more commonly referred to as controlled diffusion profiles, have been shown to feature higher efficiencies as well as a broader operability range, Hobbs & Weingold (1984). In their work, the higher performance was achieved by carefully control the pressure distribution or, equivalently, the Mach number distribution to reduce shock losses and profile losses and to avoid separation. The design approach may be categorized as either being inverse or direct. The basis of the inverse technique is to prescribe a certain flow property such as the pressure distribution around the blade and by applying an inverse design code; the corresponding blade shape can be calculated as is presented in the work of van Rooij *et al.* (2007). One of the disadvantages of designing blades with the target of meeting a certain pressure distribution is the difficulty of dealing with off-design conditions. The prescribed pressure distribution is only valid for one operating point; thus the performance at off-design conditions may not be directly controlled. The direct concept is based on defining the blade profile and in an iterative manner using the flow solver to refine the geometry until the design targets are met. The present work has considered the di-

rect approach, and the blade shapes have been parameterized with a combination of several Non-Uniform Rational B-spline (NURBS). The parameterization was developed internally prior to this work at GKN Aerospace and is based on the work by Burman (2003). The underlying theory of NURBS curves is described in depth in Piegel & Tiller (1997).

The blade profile is constructed by a camberline, a thickness distribution and a nose curve describing the leading and trailing edges. The main parameters involved are presented in Fig. 2.5. The camberline,

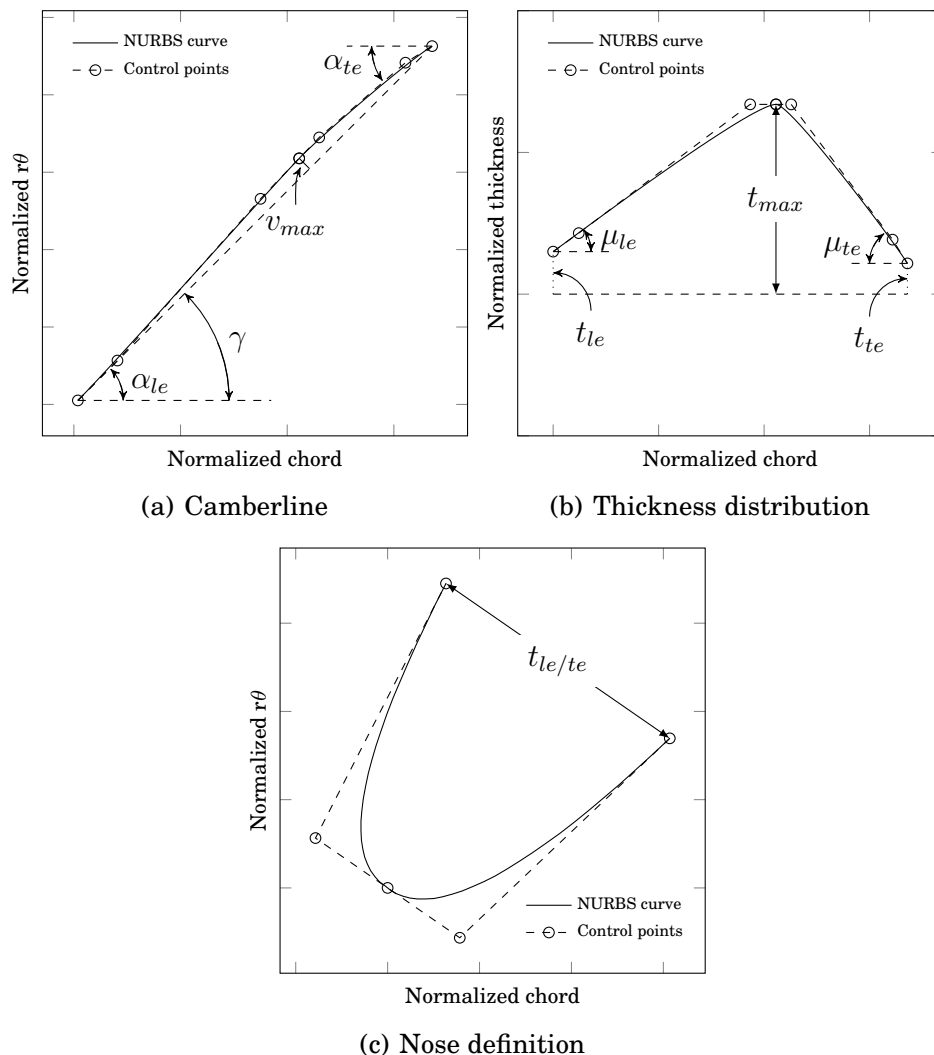


Figure 2.5: Blade construction with meanline and thickness distribution

see Fig. 2.5(a), is defined by two cubic B-splines that are connected at the position of maximum camber (v_{max}). The leading and trailing edge

angles (α_{le} & α_{te}) determine the initial and final slope of the B-splines and the stagger angle (γ) the relative position of the control points positioned at the leading and trailing edges. The thickness distribution presented in Fig. 2.5(b) is defined in a similar fashion and the two segments are joined at the position of maximum thickness (t_{max}). The slope of the thickness distribution at the leading and trailing edges are specified with the wedge angles (μ). The thickness distribution is applied along the camberline to obtain the blade suction and pressure sides. Finally, the two sides are connected with the nose curves, shown in Fig. 2.5(c), defining the leading and trailing edges. The segments share the same the slope at the transition points and thus C1 continuity is enforced.

An alternative approach that makes use of Bezier curves to define the blade shape has been developed and investigated in cooperation with GKN Aerospace during this project, see Skärnell (2011). In contrast to using a camberline and thickness distribution, the basis of this technique consists of describing the suction and pressure sides directly using 5th order Bezier curves defined by Eqn. 2.4

$$\begin{aligned} C(t) = & (1-t)^5 P_0 + 5t(1-t)^4 P_1 + 10t^2(1-t)^3 P_2 \\ & + 10t^3(1-t)^2 P_3 + 5t^4(1-t) P_4 + t^5 P_5, \quad t \in [0, 1]. \end{aligned} \quad (2.4)$$

where P represents the control points and t the normalized length parameter. An example of two Bezier curves is illustrated in Fig. 2.6. The

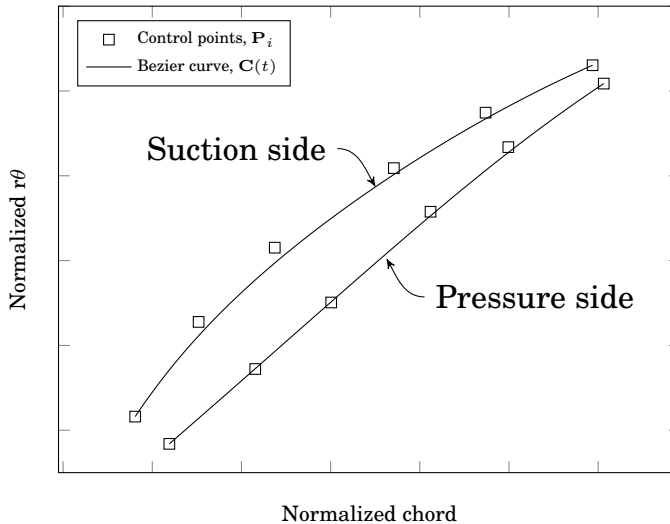


Figure 2.6: Pressure and suction sides described by 5th order Bezier curves

leading and trailing edges are constructed with 6th order polynomials

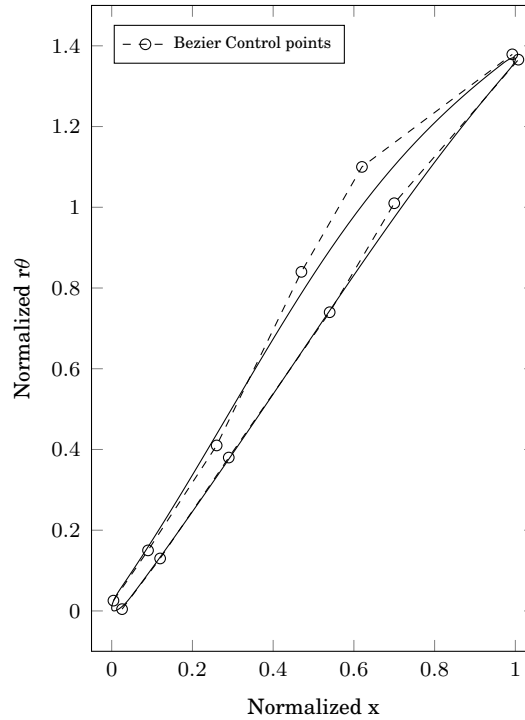


Figure 2.7: Profile constructed both from Bezier curves and cubic B-splines

in order to obtain a continuous curvature (C2 continuity) at the transition points. The advantage of this approach is that the suction and pressure sides can be designed independently, and this offers a higher dimensional space compared to the more traditional cubic parameterization. Furthermore, leading edge spikes as discussed in Goodhand & Miller (2010), or other sudden pressure jumps related to discontinuous curvature that may trigger a flow separation, are avoided since the curvature is smooth. From a practical point of view, the disadvantage of this type of approach is that the blade thickness can not be directly specified so additional thickness constraints must be considered. Also, as discussed in Piegl & Tiller (1997), compared to B-splines properties, a displacement in one control point changes the curve globally. Thus, when working with Bezier curves, it is more difficult to change a geometry locally. An example of a blade profile generated by both the Bezier and B-spline methods is illustrated in Fig. 2.7. The 2D profile seen in Fig. 2.7 lies in the blade-to-blade plane along a streamline. This is an important feature as the requirements set on a blade profile are taken from the performance along a specific streamtube consistent with the streamline curvature analysis. The profiles at different streamlines are then stacked onto a stacking line which may be defined by a Bezier or B-spline curve. The stacking line can be used to move the profiles

relative to each other to produce a combination of sweep, shown in Fig. 2.8(a), and lean, shown in Fig. 2.8(b). Two examples of stacked profiles

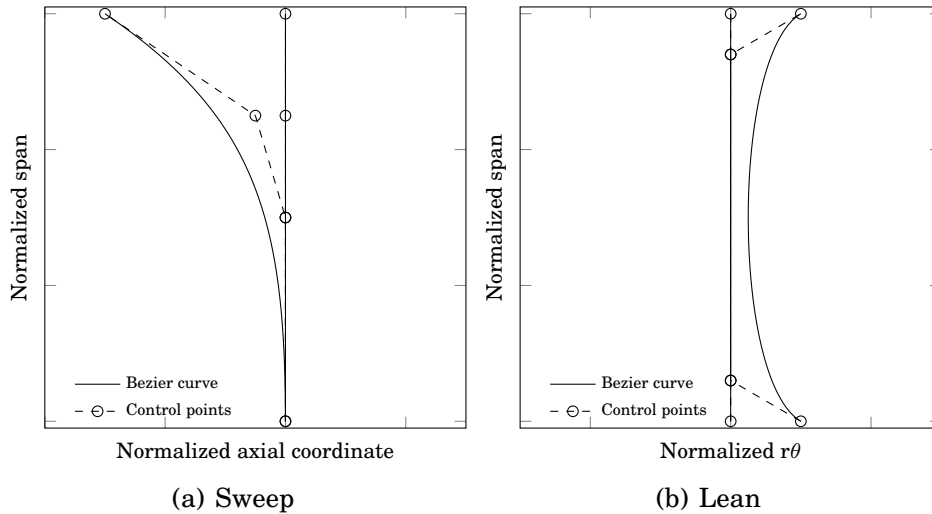


Figure 2.8: Examples of different stacking lines

along the stacking line are illustrated in Fig. 2.9. A front swept rotor

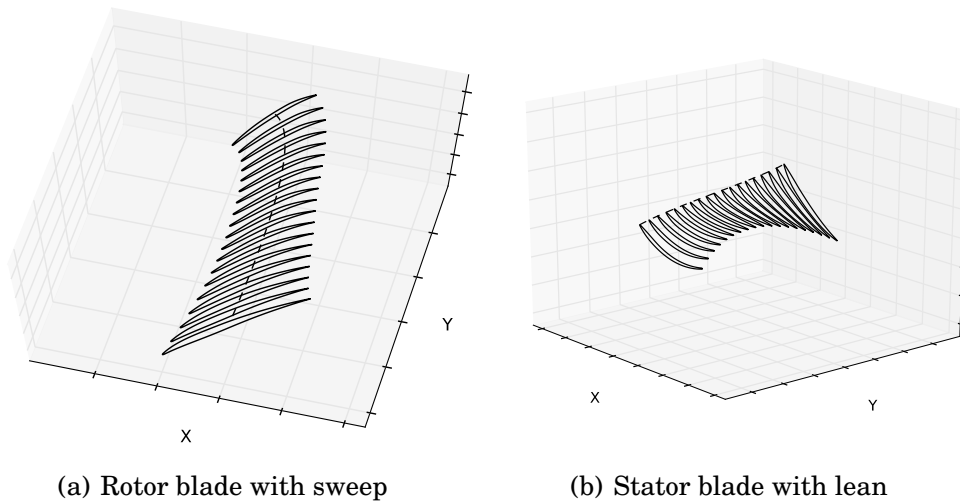


Figure 2.9: Examples of 3D blades

blade is shown in Fig. 2.9(a), while a stator blade with lean is shown in Fig. 2.9(b).

Chapter 3

CFD modeling

3.1 Governing equations

The CFD solver used for design and analysis is based on the compressible RANS equations with the realizable k - ε turbulence model expressed in compact form in Eqn. 3.1

$$\frac{\partial Q}{\partial t} + \frac{\partial \mathcal{F}_j}{\partial x_j} = \mathcal{H} \quad (3.1)$$

The state vector, Q , is defined as

$$Q = \begin{bmatrix} \bar{\rho} \\ \bar{\rho} \tilde{u}_i \\ \bar{\rho} \tilde{e}_0 \\ \bar{\rho} \tilde{k} \\ \bar{\rho} \tilde{\varepsilon} \end{bmatrix} \quad (3.2)$$

The flux vector is expressed as

$$\mathcal{F}_j = \begin{bmatrix} \bar{\rho} \tilde{u}_j \\ \bar{\rho} \tilde{u}_i \tilde{u}_j + \bar{p} \delta_{ij} - \tau_{ij} \\ \bar{\rho} \tilde{e}_0 \tilde{u}_j + \bar{p} \tilde{u}_j - C_p \left(\frac{\mu}{Pr} + \frac{\mu_t}{Pr_t} \right) \frac{\partial \tilde{T}}{\partial x_j} - \tilde{u}_i \tau_{ij} \\ \bar{\rho} \tilde{k} \tilde{u}_j - \left(\mu + \frac{\mu_t}{\sigma_k} \right) \frac{\partial \tilde{k}}{\partial x_j} \\ \bar{\rho} \tilde{\varepsilon} \tilde{u}_j - \left(\mu + \frac{\mu_t}{\sigma_\varepsilon} \right) \frac{\partial \tilde{\varepsilon}}{\partial x_j} \end{bmatrix} \quad (3.3)$$

and the source vector (\mathcal{H}) includes the production and dissipation of k and ε defined as

$$\mathcal{H} = \begin{bmatrix} 0 \\ 0 \\ 0 \\ P_k - \bar{\rho}\tilde{\varepsilon} \\ (C_{\varepsilon 1}P_k - C_{\varepsilon 2}\bar{\rho}\tilde{\varepsilon})\frac{\tilde{\varepsilon}}{k} \end{bmatrix} \quad (3.4)$$

The turbulence production term (P_k) is modeled as

$$P_k = \left(\mu_t \left(2\tilde{S}_{ij} - \frac{2}{3} \frac{\partial \tilde{u}_k}{\partial x_k} \delta_{ij} \right) - \frac{2}{3} \bar{\rho} \tilde{k} \delta_{ij} \right) \frac{\partial \tilde{u}_i}{\partial x_j} \quad (3.5)$$

where the coefficients $C_{\varepsilon 1}$ and $C_{\varepsilon 2}$ are constants. The density ($\bar{\rho}$) and pressure (\bar{p}) are ensemble averaged while the velocity vector (\tilde{u}_i), total energy (\tilde{e}_0), temperature (\tilde{T}), turbulence kinetic energy (\tilde{k}) and turbulence dissipation ($\tilde{\varepsilon}$) are Favre-averaged. The Reynolds stresses are modeled with the Boussinesq assumption, which implies that the viscous stress tensor τ_{ij} for a Newtonian fluid can be expressed as

$$\tau_{ij} = (\mu + \mu_t) \left(2\tilde{S}_{ij} - \frac{2}{3} \frac{\partial \tilde{u}_k}{\partial x_k} \delta_{ij} \right) - \frac{2}{3} \bar{\rho} \tilde{k} \delta_{ij} \quad (3.6)$$

where \tilde{S}_{ij} is the strain rate tensor defined as

$$\tilde{S}_{ij} = \frac{1}{2} \left(\frac{\partial \tilde{u}_i}{\partial x_j} + \frac{\partial \tilde{u}_j}{\partial x_i} \right) \quad (3.7)$$

and the turbulence viscosity (μ_t) with the realizability limiter is expressed as

$$\mu_t = \min \left(C_\mu \bar{\rho} \frac{\tilde{k}^2}{\tilde{\varepsilon}}, \frac{0.4 \bar{\rho} \tilde{k}}{\sqrt{\tilde{S}_{ij} \tilde{S}_{ij}}} \right) \quad (3.8)$$

where C_μ is a constant. The dynamic viscosity (μ) is modeled as temperature dependent following Sutherland's law. To close the system of equations it is assumed that the gas mixture is a thermally perfect gas. In other words, the internal energy and enthalpy as well as the specific heat at constant volume and pressure are described as being functions of temperature only as shown in Eqn 3.9.

$$\begin{aligned} e &= e(\tilde{T}) \\ h &= h(\tilde{T}) \\ C_v &= \frac{de}{d\tilde{T}} \\ C_p &= \frac{dh}{d\tilde{T}} \end{aligned} \quad (3.9)$$

The functions are approximated with the NASA polynomial functions described in Gordon & McBride (1994). Furthermore, the ideal gas law is used

$$p = \rho RT \quad (3.10)$$

where R is the gas constant.

3.1.1 Discretization

The spatial discretization is obtained by integrating the conservation laws in Eqn. 3.1 over a given grid cell. The convective and the diffusive fluxes are treated separately due to the different nature of these fluxes. The convective fluxes across a cell face are computed with an upwind biased third order scheme based on the method of characteristic, a theory described in Laney (1998). The upwind direction is determined by the propagation direction of the characteristic variables. The characteristic wave velocities are obtained from the linearized governing equations centered around the cell face and by considering planar waves solving for the eigenvalues of the system as described in Andersson (2005). This approach produces low numerical dissipation, however, where steep gradients of pressure and density are present; additional dissipation is artificially added, similar to Jameson & Baker (1983), to promote stability and avoid oscillations. The diffusive fluxes are obtained by computing the spatial derivatives of the primitive variables on the cell faces using a second order centered scheme. The system of equations is advanced in time using a three stage Runge-Kutta time marching method that solves the ordinary differential equation shown in Eqn. 3.11 with the time stepping scheme outlined in Eqn. 3.12

$$\frac{dQ}{dt} = F(Q) \quad (3.11)$$

$$\begin{aligned} a &= \Delta t F(Q^n, t^n) \\ b &= \Delta t F(Q^n + a/2, t^n + \Delta t/2) \\ c &= \Delta t F(Q^n + b/2, t^n + \Delta t/2) \\ Q^{n+1} &= Q^n + c \end{aligned} \quad (3.12)$$

where Δt is the time step and

$$Q^n = Q(t_n) \quad (3.13)$$

3.2 Geometry representation

The main function of the CFD solver used for optimization purposes is the ability to rank the blades in terms of performance. From this perspective, it is not strictly necessary to obtain a quantitatively correct prediction; more importantly, the solver should be capable of predicting differences in the overall performance caused by changes in the design. An important factor that influences the choice of geometry representation is the computational time. In general, the more detailed the geometry, the higher the resolution of the computational grid, which directly influences the computational time. It is therefore desirable to be able to neglect certain geometrical features that are not directly influenced by the parameterization. In the present work this includes neglecting fillets, surface roughness, seal leakages between rotating and stationary parts, stator hub clearances and rotor tip clearances. The assumption is that the influence of the neglected features in terms of overall performance is independent of the blade shape. If so, the overall trade between the selected design variables is unaffected. The idea is that once a blade shape has been defined, its performance is verified with a CFD model resolving these geometric details.

3.2.1 Tip clearance

One of the more critical questions to answer is whether or not the tip clearance should be included in the CFD model used for optimization. Including the tip clearance in the geometrical definition without adding sufficient number of cells in the tip region in order to resolve the associated flow structures will introduce noise in the objective function and can lead to difficulties in the optimization. However, if too large a number of additional cells are required to avoid the numerical noise, the constraints set on computational resources and time could be violated. On the other hand, if the clearance is neglected, the optimization might favor rotor designs that are more sensitive to the clearance flow. For instance, a tip loaded design may lead to a stronger clearance flow as it is driven to a large extent by the pressure gradient over the tip. Also, as the flow turning in the rotor tip is affected by the clearance flow, the optimization may result in stator designs that are less matched to the actual flow. These issues may cause the flow solver to fail in rating designs. A large amount of experimental and numerical studies have shown that tip leakage flow can play a significant role in compressor performance predictions, especially near stall, see for in-

stance Adamczyk *et al.* (1993), Hah *et al.* (2004) and Suder & Celestina (1996). In a recent study by Sakulkaew *et al.* (2013), the impact of efficiency for a wide range of tip clearances was studied numerically. The results showed that clearances less than 0.4% of the span have little effect on efficiency. However, for gaps in the range of 0.8%-3.4% of the span, the reduction in efficiency was close to linear. The validation work presented in Paper I and Paper VI showed that a design model where the tip clearance is neglected was capable of predicting the overall performance of three highly loaded transonic compressor cases with tip clearances smaller than 0.4% of the span. However in Paper VI an additional test case with a larger tip clearance ($\geq 1\%$ of span) was considered. The compressor performance was seen, both numerically and experimentally, to be substantially different as compared to the smaller clearance configuration. It was also noted that the results obtained for the design model incorporating the large tip clearance was relatively far from the experimental data in terms of mass flow, pressure ratio and efficiency. The results thus indicate that it is plausible to consider a zero-tip-clearance model in the optimization provided that the clearance height is small, as is the case in the design studies reported in Paper II, Paper III and Paper IV. Regarding larger clearances, additional validation is needed to ensure that the CFD model can quantitatively capture the effect of this complex flow.

3.3 Computational domain

The grids have been constructed with a general structured non-orthogonal surface-fitted multi-block mesh generator called G3Dmesh. The method is based on transfinite interpolation, outlined in Eriksson (1985). An o-grid is used to control the resolution around the blade geometry while the blade passage, and the upstream and downstream passages are resolved with h-grids, as illustrated in Fig. 3.1(a). A typical design grid for 3D calculations is shown in Fig. 3.1(b).

3.4 Boundary conditions

The computational setup for a rotor-stator configuration is sketched in Fig. 3.2. A mixed pressure boundary condition is used at the inlet, where radial distributions of P_0 , T_0 , α , β , k and ε are specified. This boundary type ensures that the inlet absolute flow angle is fixed

during the analysis. A well-posed non-reflecting (absorbing) boundary condition is used at the outlet. The boundary condition is based on the method of characteristics based on the work of Engquist & Majda (1977). An adiabatic no-slip condition is applied as the boundary condition at the walls, and the sides are set to rotational periodic.

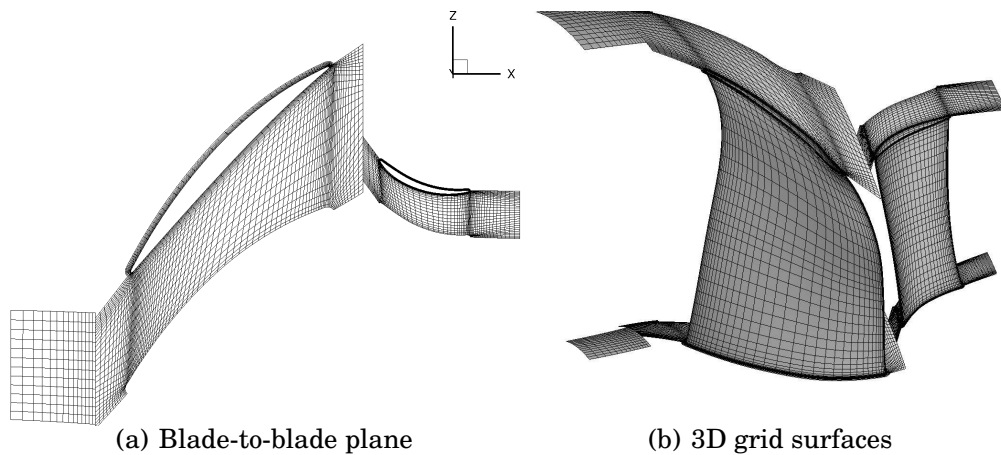


Figure 3.1: The computational grid used for CFD analysis

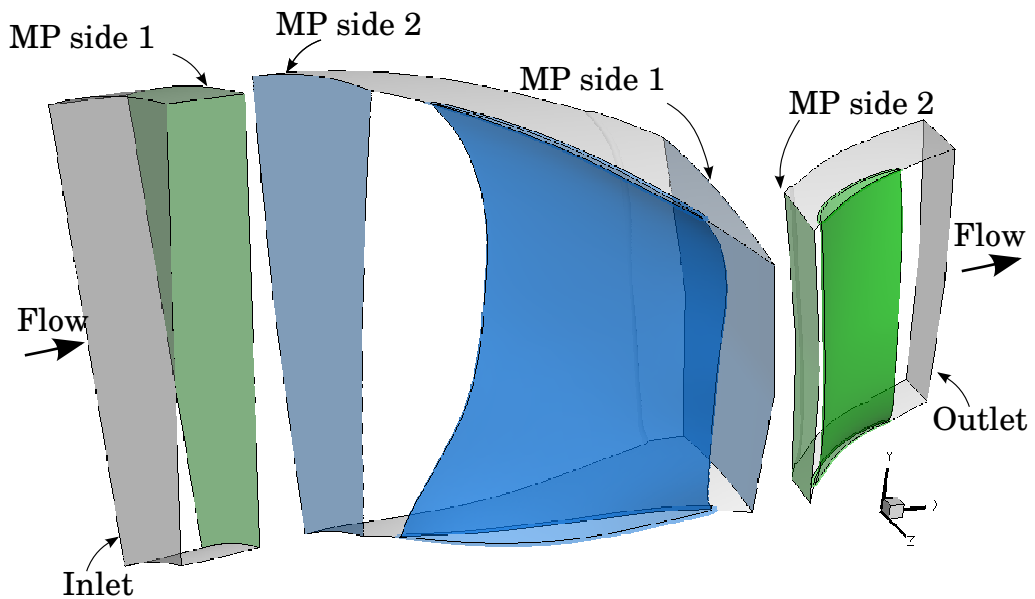


Figure 3.2: Computational setup for a rotor-stator analysis with mixing planes (MP)

3.4.1 Mixing planes

Mixing planes with non-reflective properties are used at the interfaces between the stationary and rotational domains based on the method presented in Denton (1997). The basis of the mixing plane method is to tangentially average the fluxes at each spanwise location on both sides of the interface. The fluxes are then corrected such that the two sides obtain the same average value. The flow properties downstream of the mixing plane are thus equivalent to the circumferential mixed out upstream flow. Although the model is physically sound as it conserves mass, momentum and energy, it does generate additional entropy related to the realization of losses from the mixing process. This can lead to an over-estimation of the losses since part of the wake energy originating from the upstream component may be recovered by wake stretching as it is transported through the downstream stage, a process which was originally proposed in Smith (1966) and later verified with experimental data in Zante *et al.* (2002) among others.

3.5 Mesh sensitivity study

To determine the size of the computational domain used for optimization purposes, a mesh sensitivity study was conducted in which several grid sizes reported in Table 3.1 were used to predict the overall performance of a transonic single rotor. The study was limited to include

Table 3.1: Grid sizes included in the sensitivity study

Grid name	$0.5 * Ref$	$0.625 * Ref$	$0.75 * Ref$	$0.875 * Ref$	$1.0 * Ref$	$1.25 * Ref$
Cell count	37674	68064	114720	181248	268758	521288

only grids suitable for wall functions and thus the cell sizes at the walls were kept constant to maintain a Y^+ value between 30 and 300. Figure 3.3(a) shows the variation of the predicted overall performance of the rotor in terms of pressure ratio and efficiency versus mass-flow. Even though a large variation of grid sizes was included in the study, the predictions are surprisingly similar with the exception of the near stall point, where the results obtained for the most coarse grid, $0.5x$, is seen to deviate from the more dense grids. The radial variation of the outlet flow angle is compared in Fig. 3.3(b). The differences in the predicted outlet swirl angle are mainly located in the vicinity of the 80% span, where the scatter between the most coarse and the most dense grid is about 1.5 degrees. Although local deviations can be seen, the overall

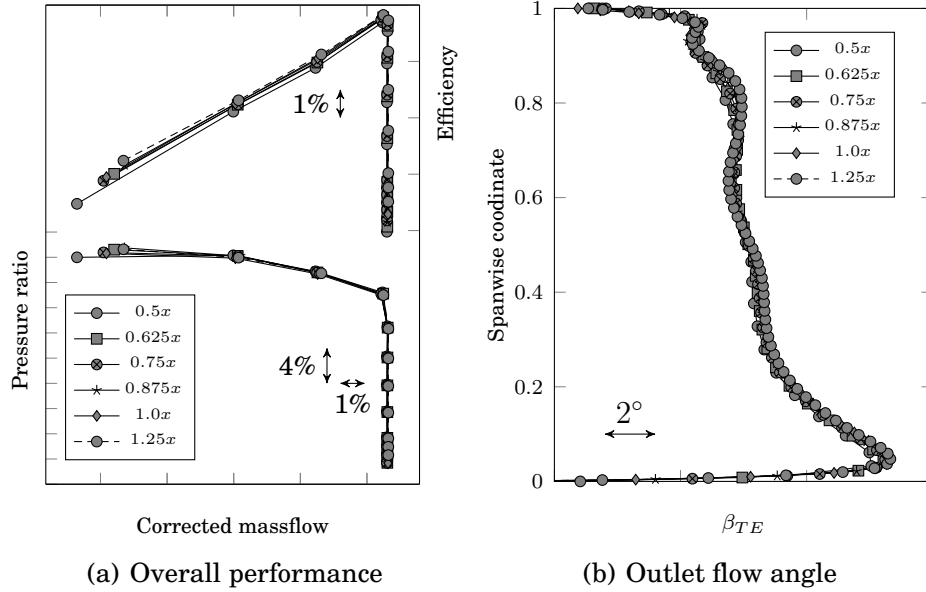


Figure 3.3: Grid sensitivity study of a single transonic rotor

radial behavior is very similar, indicating that the grid dependency is relatively small. Based on this study the grid denoted $0.625 * Ref$ was selected for optimization purposes as it provided a balance between computational cost and accuracy.

3.6 Turbulence modeling

The realizable $k-\epsilon$ model has been used in the present work in order to account for the effect of turbulence on the compressor performance predictions. It is, however, well known that the quantitative predictions are dependent on the way in which the turbulence is approximated, in particular for separated flow, as discussed in Denton (2010). The sensitivity to different turbulence modeling techniques is illustrated in Fig. 3.4 (taken from Paper VI). The figure reports the predicted performance of the 1.5 stage transonic compressor, Hulda, using the realizable $k-\epsilon$ with wall functions and the $k-\omega$ SST model with a Low Reynolds number grid. The difference in performance is small at the lower operating points but increases as the compressor reaches the stall point, i.e. as the flow separation becomes significant. However, the qualitative response of the computed total pressure and efficiency as the mass flow is varied is similar for both turbulence models. This is an important aspect of the models, as it is the ability to predict trends

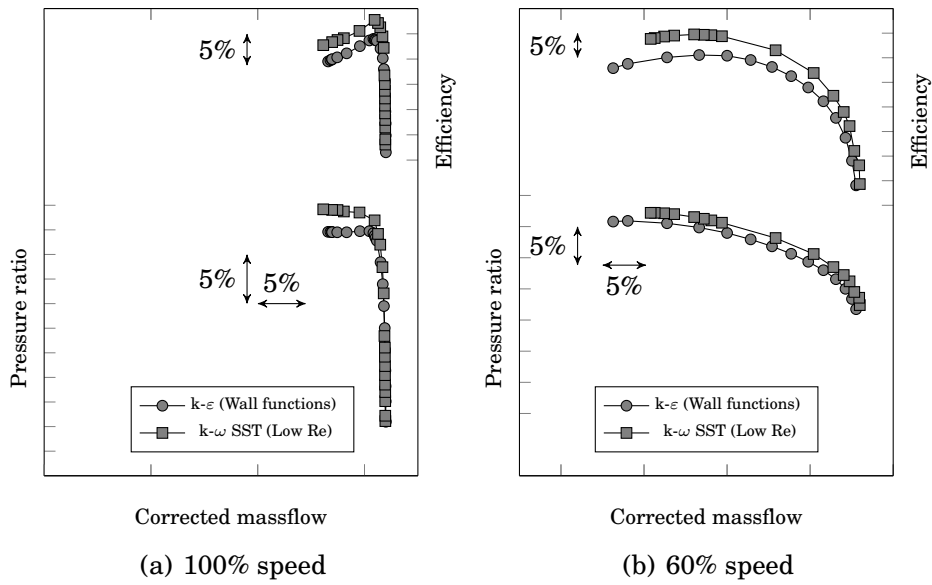


Figure 3.4: The effect of turbulence models on compressor performance

that is the most important feature for design applications and vital for a successful optimization.

Chapter 4

Optimization

OPTIMIZATION as a tool to improve a product or process is used in many forms both in industry and for academic interests. There are a vast number of different methods available, and only a brief overview is given here with an emphasis on turbo-machinery applications. The methods can be classified as either being deterministic (gradient-based) or non-deterministic.

4.1 Deterministic methods

Deterministic, usually referred to as gradient-based, methods typically use an initial design and search for improvements with the help of the gradient of the objective function, as shown in Eqn. 4.1, Vanderplaats (1984).

$$\vec{x}_{i+1} = \vec{x}_i + \alpha_i \cdot \vec{S}_i \quad (4.1)$$

where the updated design, \vec{x}_{i+1} , is based on the previous design \vec{x}_i at the i -th iteration. The change in design variables consist of the search direction, \vec{S}_i , and a scalar α_i , which defines the magnitude of the change. First order methods use the gradient as the search direction, as shown in Eqn. 4.2, where f is the objective function.

$$\vec{S}_i = -\nabla f(\vec{x}_i) \quad (4.2)$$

Second order techniques are derived from Newton's method which, in contrast to the first order methods, also uses the second derivative known as the Hessian matrix to construct a search direction, as shown

in Eqn. 4.3. Some first order methods such as the Quasi-Newton methods use this technique, but the Hessian matrix is estimated from changes in the gradient rather than being computed directly.

$$\vec{S}_i = -\frac{\nabla f(\vec{x}_i)}{\nabla^2 f(\vec{x}_i)} \quad (4.3)$$

Once the search direction (\vec{S}_i) has been selected, the optimization reduces to a line search in which the scalar α_i is optimized to provide a minimum of the objective function. The search direction is then updated, and the procedure is repeated until convergence is reached. The classic approach to obtaining the gradient information is to make perturbations of the design parameters and use the numerical solver to calculate the response of the objective function. However, if the number of design parameters is large and if the evaluation of the objective function requires a large computational effort, obtaining the gradient in this manner, and in particular the Hessian, becomes very expensive. Further difficulties computing the gradients arise if the objective function is noisy or discontinuous. An alternative technique used to obtain the gradients that has recently grown in popularity in the turbomachinery community is the adjoint method. This approach is based on deriving a sensitivity equation with respect to the objective function. Unlike the classical approach, only one adjoint solution is needed to obtain the gradient information of the objective function. This is particularly advantageous for problems with many design parameters and few objectives. The method was demonstrated by re-designing several compressor test cases, including multistage compressors, in Wang *et al.* (2010).

The gradient-based optimization methods may be very efficient. In particular the Newton's method, which only requires one iteration provided that the objective function is quadratic and convex, Vanderplaats (1984). However, unless the objective function is convex, the optimizations are likely to result in a local optima. Multi-objective optimizations are handled by re-formulating the problem into a single objective where weights are put to each objective and penalty functions are used to impose constraints. The possibility to select the best possible trade-off between the objectives is therefore limited. In spite of the drawbacks mentioned, deterministic methods have been successful in many cases such as in the work of Köller *et al.* (2000), Lee *et al.* (2001) and Wang *et al.* (2010).

4.2 Non-deterministic methods

The non-deterministic methods do not rely on gradient information and are thus able to handle noisy, discontinuous objective functions. A very popular group of methods is the evolutionary algorithms, which are inspired by evolution observed in nature. An initial population of designs is specified, and it is evolved during the optimization by adapting to the specified environment. Many different evolution strategies have been developed, but the most common is perhaps the Genetic Algorithm (GA). Each design parameter is encoded in strings of digits referred to as chromosomes, Wahde (2008). For each design in the population, the constraints and objectives are evaluated and assigned a fitness value that is later used to rate the designs. The next generation of designs is generated by means of selection, crossover and mutation. An important aspect of the selection process is its stochastic behaviour in which the likelihood of a parent to be selected is related to its fitness value, i.e. the most fit individuals are more likely to be selected but the process also permits less fitted individuals to be reproduced as well. In this way the diversity of the population can be maintained and the optimization is less likely to be trapped in a local optimum. The children are then bred by means of a crossover procedure that consists of combining a randomly selected string from the parents genes. Next, the new designs undergo a mutation process where the genes are allowed to change randomly based on a pre-defined mutation probability. While the child population may completely replace the original population, in most cases an elitism strategy is employed that prevents the best individuals of the previous generation from being lost. A key aspect of the algorithms is their stochastic behavior, which keeps the optimization from being trapped in a local optimum.

In contrast to the gradient-based methods, several objective functions and constraints may be considered separately. The optimization results in a pareto-optimal solution where the trade-off between the objective functions is available. This can then be used to select a design with an appropriate balance between the multiple objectives. The main drawback is that it requires a larger amount of function evaluations compared to the deterministic methods, and this can cause severe problems for CFD-based optimizations. This may however be remedied by the use of a meta-model assisted optimization process. Many studies have shown that meta-model assisted non-deterministic optimization methods are applicable to the design of various turbo-machinery components such as for fans in Aulich & Siller (2011), compressors in Lepot *et al.* (2011) and turbines in Song *et al.* (2011).

4.3 Selection of optimization algorithm

The main goal in the present project was to develop an efficient design procedure capable of balancing efficiency and stability. The ability to treat multiple objectives separately was therefore a desirable feature which motivated the use of genetic algorithms. An attempt was made in Paper II to optimize a single stage transonic rotor by integrating the geometry parameterization, mesh generator and CFD solver with the genetic algorithm, NSGA-II, described in Deb *et al.* (2000). This work showed promising results but it was realized that the computational effort necessary to obtain a rotor with high performance was very large. This was avoided in the work presented in Paper III, however, where the design procedure was accelerated using a meta-model.

4.4 Meta-models

Using a meta model, the computationally costly CFD simulations can be approximated with a lower order model. A set of designs with a response corresponding to that obtained by the CFD solver is used to fit a multidimensional surface describing the system behavior. The designs included in the training set are usually generated with some sort of DOE sampling such as a factorial, random or orthogonal process. The work of Simpson *et al.* (2001) provides a good summary of DOE sampling methods related to engineering design. The traditional methods used to build meta-models, described in detail in Myers & Montgomery (2002), are the least square fitting of polynomials and are typically referred to as response surface models (RSM). The advantages of the RSM are that the surface is smooth and its behavior is intuitively easy to understand. However, the shape of the surface is predefined by the degree of the polynomial, which may not describe the actual response accurately. Furthermore, the number of CFD evaluations required to build the model must be larger or equal to the number of unknown coefficients of the polynomial, and this can be a major drawback if there is a large number of input parameters. Also, since the method is based on regression, the approximate model will not necessarily be exact at the known points. Other techniques that have recently grown in popularity include the Kriging, Neural Networks and the Radial Basis Functions. Kriging has been used to accelerate an optimization procedure used to design fans described in Aulich & Siller (2011) and turbines in Song *et al.* (2011). The neural network is capable of handling very complex

non-linear systems, and several authors report good results when it has been used for turbo-machinery applications, Schmitz *et al.* (2011) and Huppertz *et al.* (2007) to name a few. Turbomachinery design processes have also been successfully accelerated using RBF, for instance in Lepot *et al.* (2011) and Pierret (2005). What is common with these methods is that they can capture complex non-linear systems and do not require a specific amount of known data points.

4.4.1 Radial Basis Functions

The method outlined in Hardy (1990) is an interpolator where an unknown point is a function of the Euclidean distance to its neighboring known points. This is expressed mathematically in Eqn. 4.4, where \hat{f} corresponds to the function estimator, c_j the coefficient vector, ϕ the radial basis function and N the number of known data points.

$$\hat{f}(\mathbf{x}) = \sum_{j=1}^N c_j \phi(r) \quad (4.4)$$

The radial basis function taken from Hardy (1990) is defined in Eqn 4.5

$$\begin{aligned} \phi(r) &= (1 + r^2)^{(1/2)} \\ r &= \|x - x_j\|/\sigma \end{aligned} \quad (4.5)$$

where $\|\cdot\|$ is the Euclidean norm, x_j the known data points and σ a fixed scaling parameter. The coefficients c_j in Eqn. 4.4 are obtained by imposing that the RBF model must go through the known values, $f(x_i)$. The system of equations can thus be expressed in matrix form as shown in Eqn. 4.6.

$$\mathbf{A} \cdot \mathbf{c} = \mathbf{f} \quad (4.6)$$

Matrix \mathbf{A} corresponds to the radial basis functions obtained from the known points

$$\mathbf{A} = (1 + (\|x_i - x_j\|/\sigma)^2)^{(1/2)}, \quad i, j \in [1, N]. \quad (4.7)$$

Given that matrix \mathbf{A} is non-singular, the vector \mathbf{c} can be obtained by inverting the linear system of equations according to Eqn. 4.8.

$$\mathbf{c} = \mathbf{A}^{-1} \cdot \mathbf{f} \quad (4.8)$$

4.5 On the selection of meta-model

Regarding turbo-machinery applications such as the design of a transonic compressor it was seen that models that can cope with discontinuities are more likely to be able to characterize the shape of the objective function. To illustrate this, the results of a study made at GKN Aerospace prior to this project are presented below. The focus of the study was to determine whether a second order polynomial function could be used to describe the pressure loss of a 2D compressor profile with respect to a change in stagger angle. The results are shown in Fig. 4.1(a). It reports the CFD predicted pressure loss (ω) as a function of a

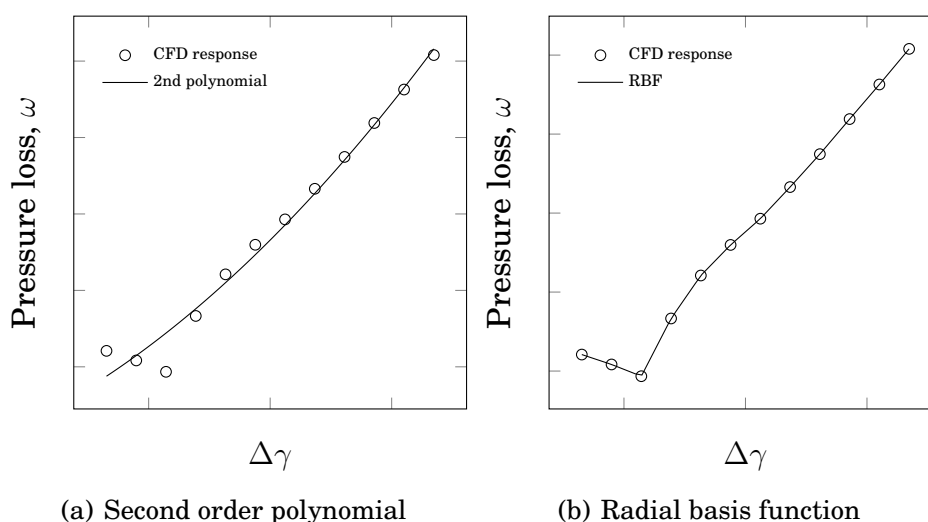


Figure 4.1: Pressure loss as a function of stagger angle approximated by meta-models

change in the stagger angle ($\Delta\gamma$) as well as the response approximated by a second order polynomial function. The CFD predicted response shows a clear discontinuity in the left region of Fig. 4.1(a). As the stagger angle increases, the sudden jump in pressure loss was seen to be caused by the shock going from a multiple weak system of shocks to a single normal shock ahead of the blade passage with a significantly higher loss. It was also clear that the second order polynomial function was not able to reproduce this feature and, if used for optimization purposes, would fail to obtain the optimal design. To illustrate the advantages of the advanced meta-models, an RBF model was fitted to the CFD response. The result is reported in Fig. 4.1(b). For this particular test case, the RBF is clearly superior to the second order polynomial model provided that enough data points are available in the vicinity of the discontinuous region. In Paper III additional models such as the

Kriging and the Neural Networks were examined specifically for the optimization framework developed in this project. The conclusion from the study was that the Radial Basis Functions were the best approximation to the CFD response.

4.6 Developed optimization framework

The optimization framework developed during the present work is illustrated in Fig. 4.2. The first step is to generate an initial training set

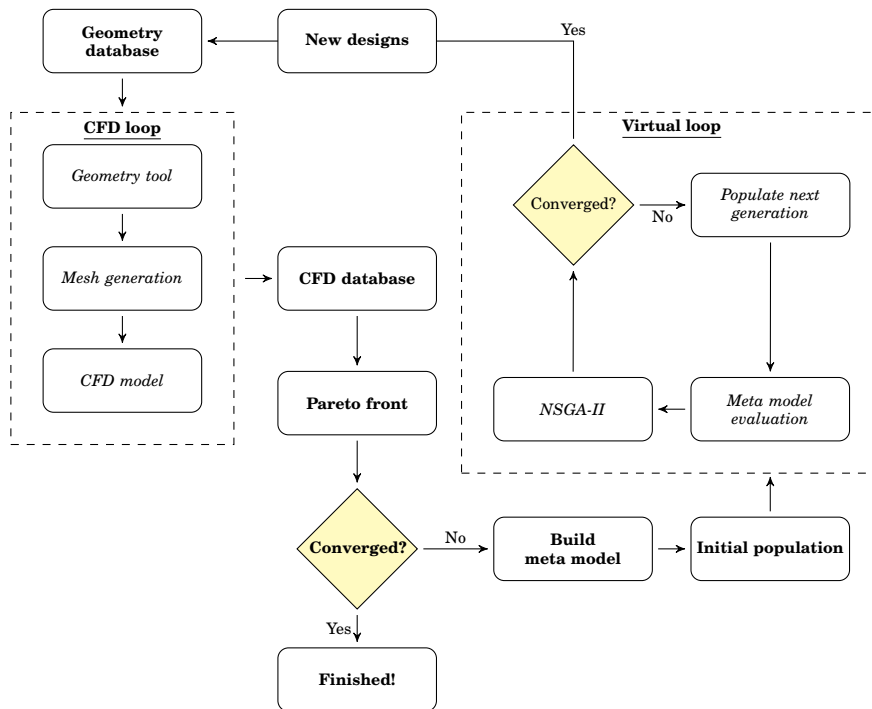


Figure 4.2: Optimization framework

with a variety of blade shapes. The number of initial designs should be chosen on the basis of the number of selected design parameters. The objective functions and constraints are then obtained in the CFD loop shown in Fig. 4.2. This process is automatic and is connected to a cluster to allow for parallel runs. Once the response has been obtained, the CFD database is used to extract the pareto-front. The meta-model (RBF) is then created based on the CFD database, and the initial population for the virtual loop is generated. The genetic algorithm (NSGA-II) is then used to search for the pareto-optimal solutions. Note that the optimization is virtual, i.e. the objectives and

constraints are approximated with the meta-model, which results in a very fast process and is normally completed within seconds. The resulting virtual pareto-front is examined, promising candidates are added to the geometry database and the CFD loop is used to obtain their true response. The CFD database is thus updated and a new pareto-front is obtained. The process then continues with an additional virtual optimization using the updated meta-model. The CFD database gradually grows and the meta-model, being exact at the known points, becomes more accurate, in particular in the region where the pareto-front lies. Eventually the updated CFD-based pareto-front has stabilized and the optimization is said to be converged.

Chapter 5

Summary of Papers

THIS chapter gives a brief summary of the results reported in the seven papers on which this thesis is based.

5.1 Paper I

L. Ellbrant, L-E. Eriksson and H. Mårtensson, 2011, CFD Validation of a High Speed Transonic 3.5 Stage Axial Compressor, *20th ISABE Conference, ISABE-2011-1226*, September 12-16, Gothenburg, Sweden

5.1.1 Division of Work

My contribution, besides being the lead author, was to build the CFD models and perform the simulations as well as the validation. Together, the co-authors supervised and provided support with regards to the solver, analysis and writing. The experimental data of the Blenda compressor were provided by GKN Aerospace Engine Systems.

5.1.2 Results and Discussion

This paper presents a simplified CFD model intended to be used for design purposes. Two key factors that influence the choice of method are the computational time required and the model accuracy. To this end a simplified CFD model was built that was fast enough to be suitable for being used as a design tool. To ensure that the suggested model

was sufficiently accurate it was used to predict the performance of a single transonic rotor in isolation and a transonic three stage compressor. The comparison between the computed results and measurements for the two test cases showed that the model can predict the overall performance with an acceptable error margin. The predictions were further verified with a detailed model using a higher resolution grid including tip clearance. This comparison showed that the variation of the total pressure ratio and efficiency with mass flow was qualitatively very similar although the more detailed model with tip clearance predicted a reduced choke mass flow and stall margin for both test cases. It was concluded that the proposed simplified model was suitable to be used for design provided that a safety margin for choke mass flow and stall margin is considered.

5.2 Paper II

L. Ellbrant, L-E. Eriksson and H. Mårtensson, 2012, Design of Compressor Blades Considering Efficiency and Stability Using CFD Based Optimization, *Proceedings of ASME Turbo Expo, GT2012-69272*, June 11-15, Copenhagen, Denmark

5.2.1 Division of Work

My contribution, besides being the lead author, was to implement the optimization procedure, perform the optimization and carry out the analysis. Together, the co-authors supervised and provided support with regard to the analysis and writing.

5.2.2 Results and Discussion

The aim of Paper II was to build a CFD based optimization platform where efficiency and stability could be balanced. This was done by connecting the blade parameterization, mesh generator and CFD solver with the optimization framework modeFRONTIER™. The CFD model was selected on the basis of the results of Paper I. The basis of the design approach was to obtain an initial 3D geometry prior to the 3D optimization by first optimizing the blade profiles at 10%, 50% and 95% spanwise positioned streamtubes using a Q3D solver. The optimization consisted of minimizing the total pressure loss coefficient at the design

point as well as maximizing the stability at part speed. The stability was quantified with the use of the static pressure recovery coefficient (C_p). The methodology was verified by re-designing the first stage transonic rotor of the 3.5 stage compressor Blenda. The results showed that the proposed optimization approach successfully obtained both profiles and 3D geometries with higher stability compared to the benchmark rotor. It was realized however that the process needed to be further refined, in particular regarding two aspects. First, the solutions obtained with the Q3D method were seen to be relatively far from the actual 3D flow. This led to an initial 3D geometry with a 5% lower mass flow rate than intended. Secondly, it was realized that the optimization process required a large number of CFD evaluations before convergence was obtained.

5.3 Paper III

L. Ellbrant, L-E. Eriksson and H. Mårtensson, 2012, CFD Optimization of a Transonic Compressor Using Multiobjective GA and Metamodels, *28th ICAS Conference*, September 23-28, Brisbane, Australia

5.3.1 Division of Work

My contribution, besides being the lead author, was to set up the test case, compare the performance of the various meta-models, build the design procedure and perform the optimization. The co-authors supervised and provided support with regard to the writing.

5.3.2 Results and Discussion

The aim of this paper was to improve the design methodology developed in Paper II by implementing a meta-model assisted optimization. The first step in this work was to evaluate the performance of the most commonly used meta-models. The second order polynomial RSM, the Radial Basis functions, the Kriging and the Neural Networks were all used to assist in the optimization of a 2D transonic compressor profile. By comparing the maximum and averaged prediction error of the meta-models, it was seen that the Radial Basis functions were closest to the CFD response. This model was then used to re-optimize the transonic rotor case considered in Paper II. The results showed that a significant

reduction in computational time was possible by introducing the meta-model in the optimization. The meta-model also allowed for a larger design space, which led to an improved compressor performance compared to the results in Paper II.

5.4 Paper IV

L. Ellbrant, L-E. Eriksson and H. Mårtensson, 2013, Balancing Efficiency and Stability in the Design of Transonic Compressor Stages, *Proceedings of ASME Turbo Expo, GT2013-94838*, June 3-7, San Antonio, Texas, USA

5.4.1 Division of Work

My contribution, besides being the lead author, was to improve the design methodology by modifying the Q3D optimization and making the necessary adjustments to allow for simultaneous optimization of the rotor and the stator. The co-authors supervised and provided support with regard to the new Q3D approach and assisted with the writing of the paper.

5.4.2 Results and Discussion

The objective of the work, that led to this paper, was to further improve the design procedure by refining the Q3D method. As mentioned in the discussion of Paper II, the original Q3D approach did not fully capture the streamtube flow which led to initial 3D blades that were quite far from the desired 3D performance, in particular with respect to the design mass flow. The idea to resolve the streamtube channel in 3D was then introduced to more accurately capture the effect of the radial variation. The solutions could then be obtained with the 3D solver, which also made it possible to consider both the rotor and the stator simultaneously since mixing planes were readily available. The design procedure was thus improved in two ways, first the Q3D method was improved and secondly the new method allowed for a rotor-stator optimization. The method was verified by re-designing the first stage of the transonic three stage compressor Blenda. The new Q3D approach showed significant improvements compared to the previous method in

that the initial 3D stage was much closer to the desired 3D design targets in terms of design mass flow. The optimization also showed that the optimized 3D stage obtained a higher part speed stability with a maintained design point efficiency compared to the original stage. By analyzing the optimized stage in the multistage environment, it was also possible to verify that the improved part speed stability of the stage also resulted in a higher stability of the whole compressor, indicating that the stage-by-stage design approach is feasible.

5.5 Paper V

L. Ellbrant, L-E. Eriksson and H. Mårtensson, 2013, Aerodynamic Properties of Novel Compressor Blade Shapes, *21st ISABE Conference, ISABE-2013-1103*, September 9-13, Busan, Korea

5.5.1 Division of Work

My contribution, besides being the lead author, was to design the two rotor geometries and perform the analysis. The co-authors supervised and provided support with regards to the analysis and the writing of the paper.

5.5.2 Results and Discussion

In this paper, the trade-off between design point efficiency and part speed stability with respect to blade parameterization was investigated in detail. Prior to this work, an optimization of a transonic stage with a large design space resulted in a novel shaped rotor featuring a trailing edge cusp at the blade tip. It was not clear why the optimization favored these types of blade shapes, but initial comparisons between this rotor and the optimized rotor in Paper IV showed that the novel blade shape did have higher stability with relatively modest penalties in design point efficiency. The numerical investigation and findings were described in this paper. In short, the trailing edge cusp essentially increases the blade discharge area and thus results in a local increase of the blade loading at the trailing edge. This is advantageous at part speed because it reduces the incidence angle at a given throttle setting, keeping the flow at the leading edge from separating and thereby improving the stability. The reason why this blade feature only resulted

in a modest penalty in design point efficiency was that the change appeared locally at the trailing edge where the flow is subsonic and so did not affect the shock losses, which is the main loss source for this type of compressor. The modest drop in design point efficiency, as reported in the paper, was a result of the rapid area increase that resulted in an increased boundary layer thickness and a small flow separation locally at the trailing edge.

5.6 Paper VI

L. Ellbrant, L-E. Eriksson and H. Mårtensson, 2014, Predictive Capability of CFD Models for Transonic Compressor Design, *Proceedings of ASME Turbo Expo, GT2014-27019*, June 16-20, Düsseldorf, Germany

5.6.1 Division of Work

My contribution, besides being the lead author, was to build the CFD models and perform the simulations as well as the validation. Together, the co-authors supervised and provided support with regard to the analysis and the writing of the paper. The experimental data of the Hulda compressor were provided by GKN Aerospace Engine Systems.

5.6.2 Results and Discussion

This paper deals with additional validation of the selected design method. In contrast to Paper I, this work also focuses on validation of part speed performance. The test compressor is a highly loaded transonic 1.5 stage compressor named Hulda. The test includes measurements from a rotor with a small tip clearance ($< 0.4\%$ of span) as well as a large tip clearance ($\geq 1\%$ of span). Additional comparisons were made with higher complexity CFD models accounting for the rotor-stator interaction. The comparison between the predictions of the design method and the measurements from the compressor test configuration with the small tip clearance was deemed to be satisfactory in terms of the variation of the total pressure ratio and efficiency as a function of mass flow. The relative change in the radial distribution of the total pressure downstream of the rotor as the throttle valve is incrementally closed

was also seen to be qualitatively well predicted when compared with the measurements. As the experimentally determined performance of the large tip clearance configuration was significantly different, a design model resolving the tip clearance was analyzed. This model was able to predict trends but was less valid in terms of a quantitative comparison. In light of the results reported in this paper, it seems necessary to do more validation and CFD development specifically aimed at improving the predictions of compressors with large tip clearances.

5.7 Paper VII

L. Ellbrant, L-E. Eriksson, 2014, General 3D Streamtube Solver, *Internal report*, Dept. of Applied Mechanics, Chalmers University of Technology, Gothenburg, Sweden

5.7.1 Division of Work

My contribution, besides being the lead author, was to implement the new Q3D approach, generate the test cases and perform the comparative study between the Q3D and the 3D results. L-E Eriksson formulated the source term and assisted in the implementation of it as well as in the writing of the paper.

5.7.2 Results and Discussion

This report describes a new solver that can be used to predict the flow in a thin annular streamtube with varying radius and area. This Q3D solver was originally used in Paper IV to optimize blade profiles along streamtubes in a rotor-stator configuration. In the original grids, however, three cells were required radially in order to obtain an accurate estimate of the radial pressure gradient present in the flow due to the radius of curvature along the streamtube and the swirling flow component. It was however realized that this method could be made more efficient. The idea was to reduce the computational domain to a single cell layer grid provided that a source term was implemented that could represent the effect of the radial pressure gradient. The formulation and implementation of the source term is contained in this report, and the accuracy of the approach is assessed with the help of two

fundamental test cases in which the solution could be described by analytical expressions. The solver is also used to predict the flow of the NASA Rotor 67 test case as well as the three stage transonic compressor Blenda. The comparison with the full 3D solutions showed that the new Q3D solver was able to predict the compressor performances and the detailed flow pattern within a reasonable accuracy, provided that the selected streamtubes are close to those obtained from tangentially averaged 3D flow fields.

Chapter 6

Concluding Remarks

THE main goal of this work has been to develop an efficient CFD-based design procedure for transonic compressor stages. The focus has been to develop and validate the CFD model used to obtain the response of the design space, construct an efficient design strategy, develop an efficient multi-objective optimization framework and verify the design procedure.

6.1 Validation

The CFD model used to rate the performance of the designs has been developed by considering a balance between sufficient accuracy and computational cost. To fulfill the constraints imposed by the computational resources, a steady RANS model with mixing planes between the blade rows was considered. The size of the computational grids was selected on the basis of a mesh sensitivity study limited to grids suitable for using wall functions. This model was then validated (Paper I and Paper V) by using experimental data measured from a single rotor in isolation, a 1.5 stage compressor and a 3.5 stage compressor, all being transonic highly loaded designs. The model was seen to be able to predict the overall compressor characteristics in terms of the variation of the total pressure ratio and efficiency with mass flow. The conclusion from this observation is thus that the model developed is capable of rating different designs, which makes it suitable as a design model in an optimization. The accuracy of this model was however seen to be limited to test cases with relatively small tip clearances. This was observed by comparing the predictions with the experimental data obtained from the 1.5 stage compressor featuring a tip clearance larger

than 1% of span. Including this tip clearance in the design model improved the qualitative accuracy, but large deviations were observed in terms of a quantitative comparison.

6.2 Design procedure

The design procedure outlined in the present work is to consider two sets of optimizations. The first step involves optimization of 2D profiles along the span based on a Q3D solver. This is used to provide an initial 3D blade upon which the 3D optimization can be based. Since the Q3D solver is much faster, a relatively large set of parameters can be used as design variables. In the 3D-design phase, the design space may then be reduced, which consequently keeps the computational resources needed within reasonable limits. This procedure was seen to work very well provided that the Q3D solver is a fair approximation to the 3D flow field. This was however not the case in the initial work presented in Paper II due to the neglected radial variation along the streamtube. A new Q3D approach was therefore suggested in which the blade-to-blade flowfield was computed with the 3D solver where the 3D streamtube shape was fully resolved (Paper IV). The improved solver led to an initial 3D blade much closer to the 3D targets. Additional improvements were later presented in Paper VII, where a source term was used to represent the pressure gradient normal to the flow path in the meridional plane. The new approach effectively reduced the Q3D computational grid to a single cell layer grid and thus led to a more efficient solver. The work also showed that the performance predicted by the new Q3D approach was representative of the full 3D flow.

6.3 Optimization

The genetic algorithm selected was seen to be robust and offered an easy way to account for two objectives and multiple constraints. The static pressure recovery used to represent stability proved to work well. Designs featuring high static pressure recovery were seen to show both higher pressure ratio capability as well as a larger flow range. Resolving the pareto-front was highly desirable, as the trade-off between the efficiency and stability could be used to find a well balanced design. Furthermore, the pareto-front offers a set of solutions rather than one

single design. The design procedure is thus robust in the sense that, if any aerodynamic or geometrical requirement is changed during an ongoing project, the pareto-front and its underlying database can be used to efficiently find a valid alternative design. The pareto-front may also assist the designer to a greater understanding of how changes in the geometry affect the trade-off between the objectives. Such an analysis was made in Paper V where a high efficiency blade was compared with a high stability blade in detail. The results of the study showed that the blade shape downstream of the throat of a transonic rotor can be adjusted to improve stability at part speed with a reasonably low efficiency penalty at the design speed. The main disadvantage of a pure genetic algorithm optimization is that an unrealistic number of computational evaluations are required. This was circumvented by incorporating a meta-model (Paper III), which significantly reduced the total design.

6.4 Future work

Robust optimization in terms of accounting for producibility and uncertainties in boundary conditions would be appealing to investigate. This could potentially lead to a more global optimum and reduce the performance sensitivity with respect to real geometry effects and uncertainties in the environment within the engine.

Extended optimization would be interesting to study in terms of optimizing all the stages in a multi-stage compressor simultaneously. This could potentially improve the stage matching and could be used as a final step once each stage has been optimized separately.

Tip clearance effects would be beneficial to study both numerically and experimentally, in particular for cases in which the tip gap size exceeds 0.4% of the span. This could lead to an improved insight into the extent to which it may be plausible to neglect the tip clearance in the design model. Furthermore it can lead to an understanding of what aspects of the CFD methodology to improve in order to model this complex flow feature sufficiently accurate.

Bibliography

- ADAMCZYK, J. J., CELESTINA, M. L. & GREITZER, E. M. 1993 The Role of Tip Clearance in High-Speed Fan Stall. *ASME Journal of Turbomachinery* **115** (1), 28-38.
- ANDERSSON, N. 2005 A Study of Subsonic Turbulent Jets and Their Radiated Sound Using Large-Eddy Simulation. PhD Thesis, Chalmers University of Technology, Gothenburg, Sweden, ISBN 91-7291-679-6.
- AULICH, M. & SILLER, U. 2011 High-Dimensional Constrained Multi-objective Optimization of a Fan Stage. In *Proceedings of ASME Turbo Expo*. Vancouver, Canada, GT2011-45618.
- AUNGIER, R. H. 2003 *Axial-Flow Compressors: A Strategy for Aerodynamic Design and Analysis*. New York: ASME Press.
- BARALON, S., ERIKSSON, L.-E. & HÅLL, U. 1998 Validation of a Throughflow Time-Marching Finite-Volume Solver for Transonic Compressors. In *Proceedings of ASME Turbo Expo*. Stockholm, Sweden, 98-GT-047.
- BÖLCS, A. & TSAMOURTZIS, V. 1991 Quasi-Three-Dimensional Characteristics Method for a Supersonic Compressor Rotor. In *Proceedings of ASME Turbo Expo*. Orlando, Florida, USA, 91-GT-81.
- BONAIUTI, D. & ZANGENEH, M. 2009 On the Coupling of Inverse Design and Optimization Techniques for the Multiobjective, Multipoint Design of Turbomachinery Blades. *ASME Journal of Turbomachinery* **131** (2), 021014.
- BURMAN, J. 2003 Geometry Parameterisation and Response Surface-Based Shape Optimisation of Aero-Engine Compressors. PhD Thesis, Luleå University Of Technology.

Lars Ellbrant, Multi-objective CFD-based design method for axial compressors

- C. H. WU 1952 A General Theory of Three-dimensional Flow in Subsonic and Supersonic Turbomachines of Axial-, Radial-, and Mixed-flow Types. *NACA TN 2604* .
- CASEY, M. & ROBINSON, C. 2010 A New Streamline Curvature Throughflow Method for Radial Turbomachinery. *ASME Journal of Turbomachinery* **132** (3), 031021.
- CUMPSTY, N. A. 1989 *Compressor Aerodynamics*. Longman Scientific & Technical.
- DEB, K., PRATAP, A., AGARWAL, S. & MEYARIVAN, T. 2000 A Fast and Elitist Multi-Objective Genetic Algorithm: NSGA-II. KanGAL Report 200001. Indian Institute of Technology Kanpur, Kanpur, PIN 208 016, India.
- DENTON, J. D. 1997 Lessons from Rotor 37. *Journal of Thermal Science* **6** (1), 1-13.
- DENTON, J. D. 2010 Some Limitations of Turbomachinery CFD. In *Proceedings of ASME Turbo Expo*. Glasgow, UK, GT2010-22540.
- DICKENS, T. & DAY, I. 2009 The Design of Highly Loaded Axial Compressors. In *Proceedings of ASME Turbo Expo*. Orlando, Florida, USA, GT2009-59291.
- ENGQUIST, B. & MAJDA, A. 1977 Absorbing Boundary Conditions for the Numerical Simulation of Waves. *Mathematics of Computation* **31** (139), 629–651.
- ERIKSSON, L.-E. 1985 Practical Three-Dimensional Mesh Generation Using Transfinite Interpolation. *SIAM Journal of Scientific and Statistical Computing* **6** (3), 712–741.
- GE Aircraft Engines 1987 *Full Scale Technology Demonstration of a Modern Counterrotating Unducted Fan Engine Concept, Design Report*. CR-180867.
- GOODHAND, M. N. & MILLER, R. J. 2010 Compressor Leading Edge Spikes: A New Performance Criterion. *ASME Journal of Turbomachinery* **133** (2), 021006.
- GORDON, S. & MCBRIDE, B. J. 1994 *Computer Program for Calculation of Complex Chemical Equilibrium Compositions and Applications*. NASA RP-1311.

- HAH, C., RABE, C. D. & WADIA, R. A. 2004 Role of tip-leakage vortices and passage shock in stall inception in a swept transonic compressor rotor. In *turbo*. Vienna, Austria, GT2004-53867.
- HARDY, R. L. 1990 Theory and applications of the multiquadric-biharmonic method. *Computers Math. Applic.* **19** (8/9), 163–208.
- HOBBS, D. E. & WEINGOLD, H. D. 1984 Development of Controlled Diffusion Airfoils for Multistage Compressor Application. *ASME Journal of Engineering for Gas Turbines and Power* **106** (2), 271–278.
- HUPPERTZ, A., FLASSIG, P. M., FLASSIG, R. J. & SWOBODA, M. 2007 Knowledge-Based 2D Blade Design Using Multi-Objective Aerodynamic Optimization And A Neural Network. In *Proceedings of ASME Turbo Expo*. Montreal, Canada, GT2007-28204.
- JAMESON, A. & BAKER, T. J. 1983 Solution of the Euler Equations for Complex Configurations. In *Proceedings of 6th AIAA Computational Fluid Dynamics Conference*. Danvers, AIAA Paper 83-1929.
- JOHNSON, I. A. & BULLOCK, R. O. 1965 *Aerodynamic Design of Axial-Flow Compressors*. NASA SP-36. NASA, Washington, D.C.
- KÖLLER, U., MÖNIG, R., KÜSTERS, B. & SCHREIBER, H.-A. 2000 Development Of Advanced Compressor Airfoils for Heavy-Duty Gas Turbines - Part I: Design and Optimization. *ASME Journal of Turbomachinery* **122** (3), 397–405.
- LANEY, C. B. 1998 *Computational Gasdynamics*. Cambridge University Press.
- LARSSON, L. 2014 Analysis of concepts to reduce the environmental impact of aviation: High propulsive efficiency engines and contrail avoidance. PhD Thesis, Chalmers University of Technology, Gothenburg, Sweden, ISBN 978-91-7597-000-4.
- LEE, Y.-T., LUO, L. & BEIN, T. W. 2001 Direct Method for Optimization Of a Centrifugal Compressor Vaneless Diffuser. *ASME Journal of Turbomachinery* **123** (1), 73–80.
- LEPOT, I., MENGISTU, T., HIERNAX, S. & VRIENDT, O. D. 2011 Highly Loaded LPC Blade and Non Axisymmetric Hub Profiling Optimization For Enhanced Efficiency and Stability. In *Proceedings of ASME Turbo Expo*. Vancouver, Canada, GT2011-46261.
- LIEBLEIN, S. 1959 Loss and Stall Analysis of Compressor Cascades. *ASME Transactions, Journal of Basic Engineering* **81** (3), 387-400.

Lars Ellbrant, Multi-objective CFD-based design method for axial compressors

- LUO, C., SONG, L., LI, J. & FENG, Z. 2009 Multiobjective Optimization Approach to Multidisciplinary Design of a Three-dimensional Transonic Compressor Blade. In *Proceedings of ASME Turbo Expo*. Orlando, Florida, USA, GT2009-59982.
- McFARLAND, E. R. 1984 A Rapid Blade-to-Blade Solution for Use in Turbomachinery Design. *J. Eng. Gas Turbines Power* **106** (2), 376–382.
- MCKENZIE, A. B. 1997 *Axial Flow Fans and Compressors: Aerodynamic Design and Performance*. Cranfield Series on Turbomachinery Technology, Ashgate Publishing Limited.
- MYERS, R. H. & MONTGOMERY, D. C. 2002 *Response Surface Methodology: Process and Product Optimization Using Designed Experiments*. 2nd ed., John Wiley & Sons, Inc. New York.
- OKUI, H., VERSTRAETE, T., DEN BRAEMBUSSCHE, R. A. V. & ALSALHI, Z. 2013 Three-dimensional design and optimization of a transonic rotor in axial flow compressors. *ASME Journal of Turbomachinery* **135** (3), 031009.
- OYAMA, A., LIOU, M.-S. & OBAYASHI, S. 2004 Transonic Axial-Flow Blade Optimization: Evolutionary Algorithms/Three-Dimensional Navier-Stokes Solver. *Journal of Propulsion and Power* **20** (4).
- PIEGL, L. & TILLER, W. 1997 *The NURBS book*. Springer-Verlag.
- PIERRET, S. 2005 Multi-objective and Multi-Disciplinary Optimization of Three-dimensional Turbomachinery Blades. In *6th World Congresses of Structural and Multidisciplinary Optimization*.
- VAN ROOIJ, M. P. C., DANG, T. Q. & LAROSILIERE, L. M. 2007 Improving Aerodynamic Matching of Axial Compressor Blading Using a Three-Dimensional Multistage Inverse Design Method. *ASME Journal of Turbomachinery* **129** (1), 108–118.
- SAKULKAEW, S., TAN, C. S., DONAHOE, E., CORNELIUS, C. & MONTGOMERY, M. 2013 Compressor Efficiency Variation With Rotor Tip Gap From Vanishing to Large Clearance. *ASME Journal of Turbomachinery* **135** (3), 031030.
- SARAVANAMUTTO, H., ROGERS, G., COHEN, H. & STRAZNICKY, P. 2009 *Gas Turbine Theory, 6th ed.*. Pearson Education Limited.

- SCHMITZ, A., AULICH, M. & NICKE, E. 2011 Novel Approach For Loss And Flow-Turning Prediction Using Optimized Surrogate Models In Two-Dimensional Compressor Design. In *Proceedings of ASME Turbo Expo*. Vancouver, Canada, gT2011-45086.
- SIMPSON, T. W., PEPLINSKI, J. D., KOCH, P. N. & ALLEN, J. K. 2001 Metamodels for computed-based engineering design: Survey and recommendations. *Engineering with Computers* **17** (2), 129–150.
- SKÄRNELL, H. 2011 Parameterization and design of transonic compressor blades. MS Thesis, Chalmers University of Technology, Gothenburg.
- SMITH, L. H. 1966 Wake dispersion in turbomachines. *J. Fluids Eng.* **88** (3), 688–690.
- SONG, P., SUN, J., WANG, K. & HE, Z. 2011 Development of an optimization design method for turbomachinery by incorporating the cooperative coevolution genetic algorithm and adaptive approximate model. In *Proceedings of ASME Turbo Expo*. Vancouver, British Columbia, Canada, GT2011-45411.
- SPURR, A. 1980 The Prediction of 3D Transonic Flow in Turbomachinery using a Combined Throughflow and Blade-to-Blade Time Marching Method. *Int. J. Heat & Fluid Flow* **2** (4), 189–199.
- SUDER, K. & CELESTINA, M. 1996 Experimental and computational investigation of the tip clearance flow in a transonic axial compressor rotor. *ASME Journal of Turbomachinery* **118** (2), 218–229.
- SWOBODA, A. K., FLASSIG, P. M. & BESTLE, D. 2008 Accelerated Industrial Blade Design Based On Multi-Objective Optimization Using Surrogate model Methodology. In *Proceedings of ASME Turbo Expo*. Berlin, Germany, GT2008-50506.
- VANDERPLAATS, G. N. 1984 *Numerical Optimization Techniques for Engineering Design: With applications*. McGraw-Hill, Inc.
- WAHDE, M. 2008 *Biologically Inspired Optimization Methods*. Ashurst Lodge, Ashurst, Southampton, UK: WIT Press.
- WANG, D. X., HE, L., LI, Y. S. & WELLS, R. G. 2010 Adjoint Aerodynamic Design Optimization for Blades in Multistage Turbomachines—Part II: Validation and Application. *ASME Journal of Turbomachinery* **132** (2), 021012–1.

Lars Ellbrant, Multi-objective CFD-based design method for axial compressors

- YOUNGREEN, H. & DRELA, M. 1991 Viscous/inviscid method for preliminary design of transonic cascades. In *AIAA, SAE, ASME and ASEE, Joint Propulsion Conference, 27th, Sacramento, CA, 12 pp. 1991*.
- ZANTE, D. E. V., ADAMCZYK, J. J., STRAZISAR, A. J. & OKIISHI, T. H. 2002 Wake recovery performance benefit in a high-speed axial compressor. *ASME Journal of Turbomachinery* **124** (2), 275–284.